An approach to treat neurological Gaucher disease: expression and purification of a human acid β-glucosidase-protein transduction domain fusion from *Pichia pastoris*

by

April Mary Goebl
B.Sc., University of Victoria, 2007

A Thesis Submitted in Partial Fulfillment
of the Requirements for the Degree of

MASTER OF SCIENCE

in the Department of Biology

Supervisory Committee

An approach to treat neurological Gaucher disease: expression and purification of a human acid β-glucosidase-protein transduction domain fusion from *Pichia pastoris*

by

April Mary Goebl
B.Sc., University of Victoria, 2007

Supervisory Committee

Dr. Francis Y. M. Choy, (Department of Biology)
Supervisor

Dr. Robert L. Chow, (Department of Biology)
Departmental Member

Dr. John S. Taylor, (Department of Biology)
Departmental Member

Abstract

Supervisory Committee

Dr. Francis Y. M. Choy, (Department of Biology)
Supervisor

Dr. Robert L. Chow, (Department of Biology)
Departmental Member

Dr. John S. Taylor, (Department of Biology)
Departmental Member

Gaucher disease (GD) is caused by an inherited deficiency of the human lysosomal enzyme acid β-glucosidase (GBA, EC 3.2.1.45). Absence of functional enzyme results in lysosomal glycolipid accumulation. This disorder primarily affects organs of the reticuloendothelial system and disease severity ranges from mild hepatosplenomegaly to extreme neurological degeneration. Disease symptoms have been shown to be greatly ameliorated by enzyme replacement therapy (ERT). Limitations to therapy include the high cost of current ERT and its inability to treat neurological symptoms. In the present study I sought to produce a GBA-fusion enzyme in an economical manner that can be used to treat neurological GD. I explored the use of *Pichia pastoris* as an economical recombinant protein expression system for production of human GBA. In addition, I synthesized a protein transduction domain (PTD)-GBA fusion protein for its potential to be used as a neurotherapeutic. The results show that GBA-PTD4 can be expressed and purified from *P. pastoris.* Hydrophobic interaction chromatography and gel filtration chromatography were successful in purifying GBA-PTD4. Further optimization of expression and purification techniques is required for effective large scale production of recombinant enzyme.

Table of Contents

List of Tables

List of Figures

Abbreviations

4MUGP	4-methyl-umbelliferyl-β-D-glycopyranoside
AOX	alcohol oxidase
BBB	blood-brain barrier
bp	base pair
BSA	bovine serum albumin
CBD	cellulose binding domain
cDNA	complementary DNA
CHO	Chinese hamster ovary
CNS	central nervous system
ddH_2O	double distilled water
DNA	deoxyribonucleic acid
dNTP	deoxy nucleotide triphosphate
DTT	dithiothreitol
EDTA	ethylenediaminetetraacetic acid
ERT	enzyme replacement therapy
FXa	Factor Xa
GBA	acid β-glucosidase gene
GBA	acid β-glucosidase protein
GD	Gaucher disease
gDNA	genomic DNA
GFC	gel filtration chromatography
HIC	hydrophobic interaction chromatography
HIS4	histidine dehydrogenase gene
IPTG	isopropyl-beta-D-thiogalactopyranoside
kb	kilobase
kDa	kiloDalton
LB	Luria-Bertani
mAb	monoclonal antibody
MD	minimal dextrose
MM	minimal methanol
mRNA	messenger RNA
Mut^+	methanol utilization plus
Mut^S	methanol utilization slow
MWCO	molecular weight cut off
NMWL	nominal molecular weight limit
OD	optical density
PCR	polymerase chain reaction
PMSF	phenylmethylsulfonyl fluoride
PTD	protein transduction domain
PVDF	polyvinylidene fluoride
REN	restriction endonuclease
RNA	ribonucleic acid
RT	room temperature

RT-PCR	reverse transcription PCR
SDS-PAGE	sodium dodecyl sulphate polyacrylamide gel electrophoresis
SRT	substrate reduction therapy
TAT	trans-activator of transcription
U	units
UV	ultraviolet
X-gal	bromo-chloro-indolyl-galactopyranoside

Acknowledgments

First and foremost I would like to acknowledge my supervisor Dr. Francis Choy for his ideas, support, encouragement and optimism. The respect that I have received from Dr. Choy has helped me immensely with my M.Sc. studies. I would also like to acknowledge my supervisory committee and external examiner for all their great ideas, questions and help. Dr. Chow provided a great DNA cloning suggestion at an opportune time, Dr. Taylor always kept me thinking by asking insightful, big-picture questions and Dr. Pearson provided many helpful thesis edits. Roderick Haesevoets and the staff at the DNA Sequencing Facility (UVic) were central to the DNA sequencing performed for this project. Tom Gore and Heather Down in the UVic Advanced Imaging Lab were very supportive and helpful with sharing their knowledge of imaging software. I would like to thank my past lab mates who trained me in the many techniques needed to complete my project: Wei Ding, Jo Crawford, and Tasha Kulai. I would also like to thank Sarah Truelson, Rebecca Jantzen, Valerie Taylor, Webby Lueng and Lin Sun for all their help and many great scientific brainstorming sessions. Thank you to Craig Hammet, Edmond Li and Alex Jack for their work on side projects in the lab. Additionally, Graeme Roche was a constant help and source of great ideas throughout my work. I also thank Ross Petersen for his insight and interest in the project, and for his critical thinking and scientific passion that has helped me immensely. I must also acknowledge my amazing family and friends for their positivity, enthusiasm and continual support.

Chapter 1 – Introduction

1.1 Gaucher disease

1.1.1 Disease classification and overview of clinical features

Gaucher disease (GD, OMIM 230800, 230900, and 231000) is a human autosomal recessive lysosomal storage disorder that affects approximately 1 in 75,000 individuals in the general population, and as many as 1 in 850 individuals in populations of Ashkenazi Jewish decent (Beutler and Grabowski, 2001). Collectively, lysosomal storage disorders are a group of diseases resulting from defects in the lysosomal breakdown of macromolecules. The inability to breakdown macromolecules, for reuse of their constituting building blocks, leads to their accumulation and results in a number of diseases (Reviewed by Neufeld, 1991). Gaucher disease, specifically, results from the accumulation of an undegraded glycolipid in lysosomes of cells of the mononuclear phagocyte system (Gaucher, 1882; Beutler and Grabowski, 2001). The present study focuses on the development of a treatment for patients suffering from Gaucher disease.

Gaucher disease can present with a number of different clinical symptoms that range dramatically in severity and time of onset. Symptoms may include enlargement of the liver and spleen, bone pain and skeletal weakness leading to frequent fractures, anemia and associated fatigue, abnormal bleeding or bruising caused by thrombocytopenia, and in some cases neurological degeneration causing mental retardation, dementia and premature death (Reviewed by Balicki and Beutler, 1995). GD has been divided into three classical clinical forms based on presence or absence of neurological involvement: type I, nonneuronopathic; type II, acute neuronopathic; and

type III, subacute neuronopathic. Type I patients do not display any neurological symptoms and can range from asymptomatic to severely disabled due to bony manifestations, hepatosplenomegaly and cytopenias. Type II patients display the most severe form of the disorder and suffer from neurological symptoms that manifest at approximately 6 months of age and that ultimately result in death around age two. Type III GD patients also experience neurological involvement but disease onset is later and life expectancy is longer than in type II patients (Beutler and Grabowski, 2001). More recently, a distinct neurological form of GD termed perinatal lethal Gaucher disease has been described. This form of GD usually presents *in utero* and results in death before or shortly after birth (Mignot et al., 2003; Eblan et al., 2005). The rigidity of the above classification of GD can at times present ambiguity in diagnosis and therefore a more fluid continuum of phenotypes has also been suggested to describe GD as a spectrum disorder (Sidransky, 2004).

1.1.2 Genetic basis of Gaucher disease

Gaucher disease results from deleterious mutations in the *GBA* gene which encodes the enzyme acid β-glucosidase (GBA, glucocerebrosidase, glucosylceramidase, EC 3.2.1.45) (Brady et al., 1965). GBA is encoded by 11 exons in a 7604 base pair (bp) gene on chromosome 1q21. The gene contains two functional ATG start sites and a 19 or 39 amino acid leader sequence (depending on the start site used) that is encoded by exons 1 and 2 (Sorge et al., 1987; Horowitz et al., 1989). The leader sequence is removed in the endoplasmic reticulum before GBA is transported to the lysosome (Kornfeld, 1986; Sorge et al., 1987).

There are close to 300 known disease causing mutations in the *GBA* gene leading to the broad spectrum of GD clinical manifestations mentioned previously (Reviewed by Hruska et al., 2008). The types of reported mutations include point mutations, insertions, deletions and recombinant alleles. Recombinant alleles result from cross over events with the *GBA* pseudogene located 16 kilobase (kb) downstream of functional *GBA* (Horowitz et al., 1989; Tayebi et al., 2003). The majority of known mutations are rare or private, while some occur with high frequency in certain populations. For example, four mutations, including N370S, L444P, ins84GG and IVS2+1, account for approximately 96 % of all mutations found in Ashkenazi Jewish populations (Beutler et al., 1992).

The severity and types of GD symptoms experienced by patients are, in part, determined by the location and nature of the mutations present in their *GBA* genes. Certain mutations are consistently associated with mild type I GD since these mutations result in GBA with residual enzyme activity (Meivar-Levy et al., 1994). Conversely, mutations resulting in completely non-functional GBA, such as recombinant null alleles, have been reported repeatedly in the most severe cases of perinatal lethal GD (Reviewed by Zay et al., 2008). In addition, some mutations have been found to cause improper folding of GBA leading to degradation, or incorrectly targeted GBA leading to endoplasmic reticulum retention (Ron and Horowitz, 2005). Observations of numerous GD patients suggest that disease severity, and the striking phenotypic diversity seen in patients is due to both genetic and environmental factors. Although a link between genotype and phenotype does exist in some cases, it is not possible to consistently predict a patient's clinical outcome based on their genotype (Sibille et al., 1993; Cox and Schofield, 1997; Sidransky, 2004; Ron and Horowitz, 2005). For example, there have

been cases of monozygotic twins with GD who have identical genotypes but display very different clinical features (Lachmann et al., 2004).

1.1.3 Biochemical basis of Gaucher disease

The mature GBA polypeptide is 497 amino acids in length and with proper N-linked glycosylation at 4 of 5 acceptor sites, a glycoprotein of 62 to 67 kiloDaltons (kDa) is formed (Erickson et al., 1985; Berg-Fussman et al., 1993). The active site of GBA was determined to be located at the C-terminal portion of the polypeptide based on experiments using a specific inhibitor of activity that covalently binds GBA (Dinur et al., 1986). Elucidation of the crystal structure for GBA provided more detailed information on the location of the catalytic site. The catalytic domain was shown to consist of a TIM barrel with two glutamate catalytic residues at amino acid positions 235 and 340, encoded by exons 7 and 8, respectively (Dvir et al., 2003). GBA functions as an intra-lysosomal membrane associated enzyme that hydrolyzes glucocerebroside (glucosylceramide) to glucose and ceramide (Glew et al., 1988). Widely distributed in mammalian tissues, glucocerebroside represents a glycosphingolipid intermediate formed in the lysosome during membrane lipid recycling (Beutler and Grabowski, 2001). GBA plays a key role in glycosphingolipid catabolism by hydrolyzing the β-glycosidic bond in glucocerebroside. Absence of functional GBA leads to the accumulation of glucocerebroside in lysosomes, and the subsequent disease phenotypes discussed above (Beutler and Grabowski, 2001). Phagocytic cells, namely macrophages and monocytes, are the primary cells affected in GD due to their role in engulfing and breaking down the components of dead and dying cells (Balicki and Beutler, 1995). The resulting lipid-filled macrophages are called Gaucher cells and represent a hallmark feature of Gaucher

disease (Gaucher, 1882). The presence of these Gaucher cells in bone marrow, liver or spleen was the original technique used to diagnose GD. However, the discovery of Gaucher-like cells in other disorders has presented limitations to this technique (Alterini et al., 1996). The current diagnosis for GD consists of an assay for GBA activity in leukocyte samples (Kampine et al., 1967; Beutler and Kuhl, 1970). Mutation analysis is often performed in conjunction with activity assay to provide information for a patient's prognosis.

1.1.4 Pathophysiology of Gaucher disease

The relationship between glucocerebroside accumulation in lysosomes and the clinical presentation and progression of GD is not fully delineated. A number of factors appear to contribute to the pathophysiology of this disease. As discussed, lipid-engorged macrophages are particularly abundant in the liver, spleen, bone and lungs of GD patients, and subsequently these are the primary organs affected. The cause of immensely enlarged visceral organs in GD is often explained as being due to the accumulated glycolipids in Gaucher cells (Sawkar et al., 2006). However, several reports state that the accumulation of lipid-engorged macrophages only accounts for a small proportion of increased organ volume, and that the majority of visceral organ enlargement is likely due to an immune response initiated by infiltrating Gaucher cells that release pro-inflammatory cytokines and chemokines (Hollak et al., 1997; Cox, 2001; Boot et al., 2004). Another major characteristic of GD that is not understood in terms of pathophysiology is bone involvement. While it is known that Gaucher cells deposit in the bone marrow (Stowens et al., 1985), it is unclear how this leads to the bony manifestations observed in GD. Examination of bone tissue in GD patients reveals a high

proportion of Gaucher cells replacing hematopoietic marrow; however, there is no evidence of bony erosion, bone resorption or decreased vascularity caused by the presence of the lipid storage cells (Stowens et al., 1985; Balicki and Beutler, 1995). While an explanation for a direct cause of bone related symptoms is still unclear, indirect mechanisms of bone degradation are being investigated. For example, the inflammatory response induced by Gaucher cells may enhance cell-mediated resorption in osteoclasts (Reviewed by Balicki and Beutler, 1995). Clearly, the immune system plays a major role in the pathophysiology of GD, and continues to be investigated in order to better understand this clinically variable disorder.

The etiology of neurological symptoms in types II and III GD is also poorly understood. It is often stated vaguely that CNS involvement is due to the presence of Gaucher cells in the brain, although various investigators have proposed more detailed hypotheses to explain neurological symptoms. For example, it has been reported that neuronal involvement in types II and III Gaucher patients is in part due to elevated levels of cytotoxic glucosylsphingosine, an alternate substrate of GBA, in the central nervous system (Nilsson and Svennerholm, 1982; Orvisky et al., 2002; Enquist et al., 2007). Research has shown that this substrate accumulates in certain brain regions of GD patients and is hypothesized to be the basis for the extensive neuronal cell death (Nilsson and Svennerholm, 1982; Beutler and Grabowski, 2001). Another hypothesis put forth is that the neuropathophysiology of types II and III Gaucher disease is caused by disruption in neuronal calcium homeostasis, initiated by accumulated glucocerebroside, causing cells to become more sensitive to agents inducing cell death (Pelled et al., 2000; Pelled et al., 2005).

Evidently, the biochemical and physiological changes that underlie GD are not always clear. It is apparent however, that the accumulation of glucocerebroside in lysosomes and the formation of Gaucher cells occurs in all patients. Therefore, treatments targeted at eliminating substrate accumulation are a major focus of current Gaucher disease therapeutic research.

1.1.5 Current treatment options for Gaucher disease

There are currently two treatments for GD. These include enzyme replacement therapy (ERT), which has been used to treat GD patients for almost 20 years, and substrate reduction therapy (SRT) which represents a newer treatment option. This thesis will focus primarily on ERT, which will be described in the next section. However, SRT treatment is available as an oral drug called miglustat, and marketed as Zavesca, that functions to inhibit the synthesis of glucocerebroside (Cox et al., 2003). Miglustat slows the formation of glucocerebroside in visceral organs but does not decrease excess substrate in the body. For this reason, SRT is only effective for patients with residual enzyme activity, or in combination with ERT (Moyses, 2003; Aerts et al., 2006).

In addition to the above two therapies, two other approaches for GD treatment are in developmental stages. Small molecule chaperone therapy is currently in clinical trials and gene replacement therapy exists in the research and development phase. Chaperone therapy was designed with the notion that a proportion of patients suffer from GD due to misfolded GBA that is not transported to the lysosomes (Yu et al., 2007a; Yu et al., 2007b). Since this mutant GBA often retains enzymatic activity the small molecule chaperone drug is designed to increase the stability of mutant GBA and allow its proper folding and transport to the lysosome (Sawkar et al., 2002; Yu et al., 2007b). Gene

replacement therapy using a retroviral vector to target *GBA* to hematopoietic stem cells has been performed in a mouse model with reported success of reversing disease symptoms (Enquist et al., 2006).

1.1.6 Enzyme replacement therapy for Gaucher disease

Enzyme replacement therapy was first proposed when it was discovered that GD results from the absence of functional GBA (Brady et al., 1965; Brady, 1966). Type I GD patients have been treated with ERT since 1991 with many positive results (Reviewed by Weinreb et al., 2002). Of significance, GD was the first disorder to be successfully treated with ERT and thus this rare disease represents a paradigm for this form of treatment that is now being used to treat a number of other genetic disorders (Reviewed by Beutler, 2006). ERT for GD is a treatment in which functional GBA is provided to patients in order to replace their mutant enzyme. Functional enzyme is given intravenously and taken up by macrophages via mannose-6-phosphate receptors. The first commercially available form of ERT for GD was alglucerase, marketed as Ceredase®, a modified GBA isolated from human placental tissue. This drug was replaced by the currently used imiglucerase (Cerezyme®), a recombinant form of human GBA expressed in Chinese hamster ovary (CHO) cells (Brady, 2003). For ERT to be successful, GBA must be targeted to macrophages via exposed terminal mannose residues (Barton et al., 1990). Without mannose residues exposed, therapeutic GBA would be rapidly taken up by hepatocytes upon intravenous injection (Brady, 2003). Therapeutic GBA therefore requires *in vitro* targeted digestion of glucosyl residues to expose terminal mannose before it can act as an effective treatment (Brady, 2003; Shaaltiel et al., 2007).

Despite major health improvements in many patients administered Cerezyme®, this treatment has several limitations. Firstly, the cost of Cerezyme® is very high, representing a constraint for populations of patients who cannot afford it. In Canada, ERT is government subsidized for patients who can benefit from it. However, it represents a financial burden on healthcare systems and becomes virtually inaccessible to patients living in countries where the treatment is not subsidized (Beutler, 2006). Treatment costs range from $150,000 to $500,000 per patient per year in the United States and Canada (Beutler, 2006). A combination of factors contribute to the high cost of Cerezyme®, including its slow and labour intensive production in mammalian cells, and the financial reality of having to distribute these production costs to a relatively small patient population (Beutler, 2006).

A second limitation of current ERT is that it is ineffective in treating neurological symptoms in types II and III GD. The blood brain barrier (BBB) prevents intravenously administered enzyme from reaching the central nervous system. Thus, the BBB represents a tremendous barrier to the effective treatment of neurological disorders. One review indicates that over 98 % of new macromolecular drugs for treatment of CNS disorders are unable to cross the BBB, rendering these drugs ineffective (Pardridge, 2006).

The two primary objectives of this research are to explore a more economical expression system for recombinant GBA and to create a GBA fusion protein capable of crossing the BBB for treatment of neurological GD. The following sections will address these two objectives.

1.2 *Pichia pastoris* as an economical expression system

The current costly treatment of type I GD uses recombinant GBA expressed in the mammalian CHO cell system. Other protein expression systems, including carrot cells, insect cells and yeast, have been explored in attempts to produce GBA in a more economical manner (Sinclair and Choy, 2002; Sinclair et al., 2006; Shaaltiel et al., 2007). Here, I explore the many advantages of a yeast expression system for production of recombinant proteins. Yeast can be cultured at relatively low cost, display fast growth rates in culture, and can be grown to high cell densities (Reviewed by Gellissen et al., 1992), making such a system particularly advantageous for large scale protein production. In addition, yeast possess the post-translational machinery that allows proper folding and processing of eukaryotic proteins (Reviewed by Verma et al., 1998). In the present study, we have selected the yeast *P. pastoris* for recombinant expression of GBA.

P. pastoris is an advanced, well characterized, and commonly used yeast expression system with the potential to be used in fermentor scale culturing for production of large amounts of therapeutic enzyme in an economical manner (Higgins and Cregg, 1998). Hundreds of proteins have been produced in *P. pastoris* (Reviewed by Cereghino and Cregg, 2000), including a human lysosomal enzyme deficient in a lysosomal storage disorder similar to Gaucher disease (Chen et al., 2000).

P. pastoris is unique in that it is a methylotrophic yeast that can metabolize methanol as a sole source of carbon and energy (Higgins and Cregg, 1998). This yeast contains two alcohol oxidase (AOX) genes that are necessary for methanol metabolism, *AOXI* and *AOXII*. The AOXI gene product contributes the majority of activity needed for methanol catabolism (Macauley-Patrick et al., 2005). Interestingly, it has been observed that some recombinant proteins are expressed in higher quantities when the endogenous

AOXI gene is disrupted (Paifer et al., 1994), while others express better when it is functional (Scorer et al., 1993). Two distinct phenotypes, in terms of growth on methanol, result from the presence or absence of functional *AOXI*. Cells with intact *AOXI* grow efficiently on methanol and are termed methanol utilization plus (Mut^+), while cells with disrupted *AOXI* have impaired growth on methanol and are called methanol utilization slow (Mut^S) (Cereghino and Cregg, 2000). A number of commercially available *P. pastoris* strains exist, including those with either Mut^+ or Mut^S characteristics.

Previous attempts to express GBA in *P. pastoris* in our laboratory resulted in low levels of enzyme that exceeded the expected molecular weight of GBA. These results led to the conclusion that GBA was being hyperglycosylated following translation (Sinclair, 2001, PhD dissertation). Numerous reports of the tendency of yeast to add excess mannose residues to oligosaccharide side chains support this possibility (Nakamura et al., 1993; Dean, 1999; Gemmill and Trimble, 1999). Hypermannosylation of recombinant proteins expressed in yeast systems is problematic for several reasons. For example, excess nonhuman glycan structures will have adverse effects on catalytic activity and immunogenicity of human glycoproteins produced for therapeutic use (Hamilton et al., 2003). Additionally, hypermannosylation can lead to heterogeneity of expressed proteins, resulting in complications during characterization of recombinant proteins (Vervecken et al., 2004). Accordingly, several research groups have developed humanized strains of *P. pastoris* (Vervecken et al., 2004; Hamilton et al., 2006). A humanized *P. pastoris* strain produced by Vervecken and colleagues, GS115 containing pGlycoSwitchM5, was engineered to produce mammalian-like glycosylation through the

inactivation of a principle yeast gene involved in mannosylation, *OCH1f*, and overexpression of an α-1,2-mannosidase (Vervecken *et al.* 2004). In the present study, I use this humanized strain for expression of human GBA.

The *P. pastoris* expression vector used in this study was the pPIC9K vector designed for multi-copy integration of expression cassettes and secreted expression of recombinant proteins. A strong, inducible *AOXI* promoter has been incorporated into the expression vector which allows targeted integration into the genomic AOXI locus and methanol-induced high level expression (Cereghino and Cregg, 2000). The presence of an α-factor prepro-peptide (secretion signal) from *Saccharomyces cerevisiae* allows direct secretion of the expressed protein into the surrounding culture medium to facilitate harvesting and purification (Macauley-Patrick et al., 2005). Another attractive feature of pPIC9K is that it contains two selection genes, the histidinol dehydrogenase gene (*HIS4*) and the bacterial kanamycin gene. The *HIS4* gene acts as a selectable marker in histidinol dehydrogenase-deficient strains (such as GS115) grown on histidine-deficient medium while the bacterial kanamycin gene confers Geneticin® resistance in *P. pastoris.*

1.3 Treatment of neurological disease

1.3.1 The blood brain barrier

The BBB consists of a dense microvascular network of capillary endothelial cells containing tight junctions that confer high resistance to the uptake of circulating solutes. The capillary beds forming the BBB are not porous and leaky like those surrounding other organs, resulting in minimal pinocytosis in brain endothelial cells and reducing transcellular travel (Davson, 1976). In addition to serving as a physical barrier, the BBB represents an enzymatic and active efflux barrier. Endothelial cells as well as capillary pericytes in the BBB secrete various enzymes at their cell surfaces, namely peptidases

and esterases, which degrade many biomolecules approaching the endothelial barrier. The active efflux nature of the BBB is driven by protein transporters in the microvasculature that are triggered following influx of select small molecules from the blood to the brain. Once triggered, the transporters actively pump these small molecules from the brain into the systemic blood (Reviewed by Pardridge, 2002). As a result of the unique barrier properties of the BBB, only select molecules enter the brain from systemic circulation. Lipid soluble molecules smaller than 400 Da can enter the brain via non-specific lipid-mediated free diffusion (Fischer et al., 1998). In addition, select small and large molecules recognized by protein receptors on the BBB may enter the brain by carrier- or receptor-mediated transport (Triguero et al., 1990). Furthermore, research indicates some peptides and proteins may pass through the BBB by absorptive-mediated endocytosis in a process that involves cationic domains (Duchardt et al., 2007). By taking advantage of these natural modes of entry, brain-drug delivery research has developed various techniques to transport therapeutics into the brain.

1.3.2 Current treatment possibilities for neurological disease

The need for neurotherapeutics that can access the brain is evident in the great number of CNS disorders that could benefit from them, including Gaucher disease, Alzheimer's disease and other neurodegenerative disorders. One brain-drug transport strategy that essentially dodges the BBB is direct surgical delivery. This includes intra-cerebroventricular injection, intra-cerebral injection, and convection-enhanced diffusion (Pardridge, 2007). In addition to being invasive, these techniques tend to result in drug accumulation at the brain surface, limited diffusion from the depot site, and rapid clearance of the drug from the brain before diffusion into the inner parenchyma can occur

(Huynh et al., 2006). Although direct trans-cranial injection is effective for some drugs, such as those with target receptors on the brain surface, additional techniques for brain-drug delivery are needed. Attempts to deliver drugs from systemic circulation through the BBB include both chemistry- and biology-based methods. Chemistry-based techniques typically include increasing the lipid solubility of a drug to allow free diffusion through the BBB. This strategy has been effective for some small peptides, but is greatly restricted by size; chemical modification of a drug most often leads to an increase in size, which has deleterious effects on brain permeation (Fischer et al., 1998). Alternatively, biology-based techniques have been generated for delivery of larger drugs, such as peptides and proteins, to the brain. Biology-based strategies typically involve the use of recombinant DNA technology to synthesize fusion therapeutics with increased membrane transduction capabilities (Pardridge, 2006). Examples of this approach include fusion of monoclonal antibodies for brain access via endogenous BBB transporters (Zhang et al., 2002) or addition of small cationic peptides that facilitate transduction across cellular membranes including the BBB (Schwarze et al., 1999). This study focuses on the use of a small cationic protein transduction domain (PTD) as a fusion partner to recombinant GBA for its potential to transport the therapeutic enzyme across the BBB. The following paragraphs provide a more detailed review of the use of PTDs and their various successes.

1.3.3 Protein transduction domains

In 1988, it was discovered that the trans-activator of transcription (TAT) protein from HIV-I has the ability to cross biological membranes and enter cells (Frankel and Pabo, 1988; Green and Loewenstein, 1988). Soon after, it was concluded that the region

of the protein that conferred translocation is a 35 amino acid region centered on a basic domain (Fawell et al., 1994). Further studies showed that the fragment of the TAT protein that facilitates translocation is an 11 amino acid positively charged domain, rich in arginine residues (Vives et al., 1997; Schwarze et al., 1999). Additionally, studies conducted on the secondary structures of the short TAT peptides found that the presence of optimally positioned arginine residues and α–helix-promoting alanine residues are the most important aspects for transduction across biological membranes (Vives et al., 1997; Ho et al., 2001). One study looking at multiple variants of the TAT domain found that a particular domain denoted as PTD4 had the best transduction ability based on results using flow cytometry. The sequence of the PTD4 domain is YARAAARQARA (Ho et al., 2001).

PTDs have been employed as fusion partners with various small and large biomolecules to study transduction into a number of cellular targets *in vitro* and *in vivo*. Of particular significance, Schwarze et al. (1999) showed that the 120 kDa β-galactosidase enzyme could be transported by a TAT-derived-PTD into cells of various organs including the brain. This was achieved in a mouse, and the catalytic activity of β-galactosidase was not compromised (Schwarze et al., 1999). There have been numerous reports of successful PTD-facilitated drug transport, including a study in which a human lysosomal enzyme fused to PTD was transported into the brain of a mouse with a lysosomal storage disorder (Zhang et al., 2008). These studies, among others, suggest the use of PTDs as a viable option for drug delivery and we have therefore selected PTD4 as a fusion partner for GBA in this work.

1.4 Project overview

This thesis describes the research performed on heterologous expression and purification of GBA-PTD4 from *P. pastoris*. Expression of this novel fusion enzyme in a yeast system is explored as an economical approach for production of a treatment for neurological Gaucher disease.

Chapter 2 - Materials and Methods

2.1 Construction of expression vectors

2.1.1 General overview

The following DNA constructs were synthesized for this study: cellulose binding domain (an affinity purification tag) (CBD)-*GBA*, CBD-PTD4-*GBA*, CBD-*GBA*-PTD4, and *GBA*-PTD4 (Figure 2.1a). All final constructs were in the pPIC9K vector (*P. pastoris* expression vector, Invitrogen, Carlsbad, CA) (Figure 2.1b). Briefly, the CBD-*GBA* construct was made by adding the DNA sequence encoding CBD to an existing pPIC9K expression vector from our previous work containing His_6-Fxa-*GBA*. The PTD4 fusion constructs, CBD-PTD4-*GBA* and CBD-*GBA*-PTD4, were made by tailed polymerase chain reaction (PCR) amplification of *GBA* cDNA to introduce N- and C-terminal PTD4. The CBD sequence, flanked by *Eco*RI sites introduced by tailed PCR, was added later by ligation into a pPIC9K vector already containing the PTD4-*GBA* portion. Identification of mutations in the GBA cDNA portion of the above three constructs led to the construction of a mutation-free pPIC9K-*GBA*-PTD4 construct. The mutation-containing fragment of *GBA* cDNA in pPIC9K-*GBA*-PTD4 (an intermediate synthesized during the construction of pPIC9K-CBD-*GBA*-PTD4) was removed using restriction endonucleases (RENs) and replaced with an error-free copy of the same GBA fragment.

2.1.2 Details of cloning

Construct pPIC9K-CBD-*GBA* was made by addition of the CBD sequence (from exoglucanase Cex protein of *Cellulomonas fimi* donated by Dr. T. Pfeifer (University of British Columbia, Vancouver, BC)) to an existing pPIC9K-His_6-Fxa-*GBA* vector (Wei

a)

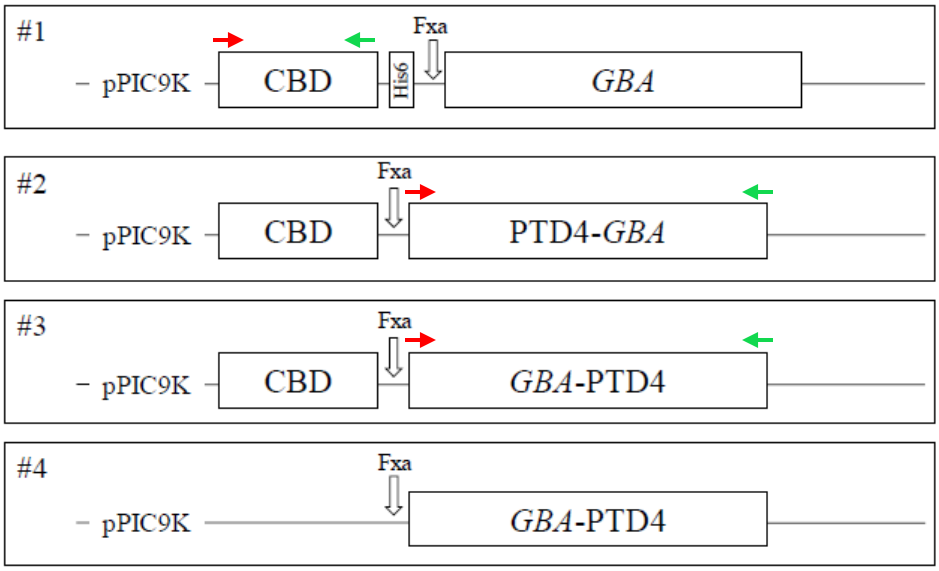

b)

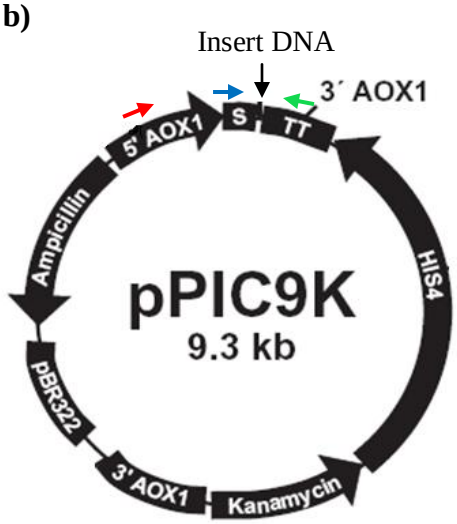

Figure 2.1 Schematic representations of a) expression constructs and b) pPIC9K vector. **a)** Schematic representation of expression constructs #1 CBD-*GBA*, #2 CBD-PTD4-*GBA*, #3 CBD-*GBA*-PTD4, and #4 *GBA*-PTD4 in pPIC9K *P. pastoris* expression vector. Primer binding locations are indicated by coloured arrows. #1: C1 (red arrow), C2 (green arrow); #2: GP1 (red arrow), G2 (green arrow); #3: G1 (red arrow), GP2 (green arrow). **b)** Schematic diagram of pPIC9K vector indicating position of expression cassette insertion. Vector specific primer binding sites are indicated by coloured arrows. 5'AOXI forward (red arrow), α-secretion signal forward (blue arrow), 3'AOXI reverse (green arrow). α-secretion signal (S). Termination of transcription signal (TT). Adapted from the pPIC9K user manual (Invitrogen, Carlsbad, CA).

Ding, University of Victoria, Victoria, BC). The Factor Xa (FXa) protease recognition site in this construct was present to allow cleavage of the affinity tags, CBD and His_6, after purification. The *GBA* cDNA sequence (generously provided by Dr. Ernest Beutler, The Scripps Research Institute, La Jolla, CA) in this and all other constructs started with the codon that encodes the first amino acid of the mature-polypeptide found in exon 3 of the gDNA sequence. The CBD sequence was amplified by tailed PCR to introduce flanking *Eco*RI sites and a 3' linker sequence, using 1x HiFi buffer, 1.5 mM $MgSO_4$, 0.25 mM dNTPs, 1 unit (U) Platinum® Taq DNA Polymerase High Fidelity (Invitrogen), and 0.4 μM of each custom, tailed primer: (Integrated Technologies Inc. San Diego, CA) C1 and C2 (Table 2.1). The incorporated linker sequence encodes a five amino acid domain (GGGGS) designed to increase the distance between the expressed CBD domain and the GBA polypeptide. Amplification was performed using a RoboCycler Gradient 40 PCR thermal cycler (Stratagene, La Jolla, CA) with 20 μl of mineral oil and the following conditions: an initial denaturation at 95°C for 5 mins, 35 cycles of 95°C for 1 min, 58°C for 1 min, and 72°C for 1 min, and a final elongation at 72°C for 5 mins. PCR amplicons along with a DNA standard (pUC Mix Marker, Fermentas, Burlington, ON) were visualized by gel electrophoresis on a 1.5% (w/v) agarose gel stained with ethidium bromide using an EpiChemi^3 Darkroom UV imager and LabWorks software (UVP BioImaging Systems).

Constructs pPIC9K-CBD-PTD4-*GBA* and pPIC9K-CBD-*GBA*-PTD4 were made in two steps. Briefly, PTD4-containing *GBA* was cloned into pPIC9K followed by CBD ligation into the expression vector. In detail, tailed primers designed to introduce the PTD4 sequence at both the N- and the C-terminus of *GBA* cDNA were used in a PCR

Table 2.1 Oligonucleotide primers used in construction of expression vectors. Primers used in amplification of CBD (C1 and C2), PTD4-*GBA* (GP1 and G2) and *GBA*-PTD4 (G1 and GP2). Primers were also used in direct colony PCRs for screening. Restriction endonuclease recognition sites are in bold print. The sequence of the five amino acid linker is in italic print. FXa recognition site is in lower case. The PTD4 sequence is underlined. Primer binding locations are shown in Figure 2.1a.

Primer name	**Primer sequence (5'-3')**	**Orientation**
C1	**GAATTC**TCCGGTCCAGCCGGCTG	Sense
C2	**GAATTC***AGATCCGCCGCCACC*TGTAGGTGAGGTAG TCGGA	Anti-sense
GP1	**GAATTC**atcgagggtagaTACGCTAGAGCTGCCGC TAGACAAGCTAGAGCTGCCCGCCCCTGCATCCC	Sense
G2	**GCGGCCGC**TCACTGGCGACGCCACAG	Anti-sense
G1	**GAATTC**atcgagggtagaGCCCGCCCCTGCATCCC	Sense
GP2	**GCGGCCGC**TCAAGCTCTAGCTTGTCTAGCGGCAGC TCTAGCGTACTGGCGACGCCACAGG	Anti-sense

reaction containing 1x HiFi buffer, 1.5 mM $MgSO_4$, 0.1 mM dNTPs, 1 U of Platinum Taq DNA Polymerase High Fidelity, and 0.3 μM of each custom tailed primer, GP1 and G2 for N-terminal fusion, and G1 and GP2 for C-terminal fusion (Table 2.1). PCR reactions were performed in a GeneAmp PCR thermal cycler (Perkin Elmer, Wellesley, MA) using the following profile: an initial denaturation at 94°C for 5 mins, 30 cycles of 94°C for 1 min, 58°C (for N-terminal fusion) or 55°C (for C-terminal fusion) for 1 min, and 72°C for 1.5 min, and a final elongation at 72°C for 5 mins. PCR amplicons were visualized by gel electrophoresis on a 1.5% (w/v) agarose gel with a 1 kb DNA standard (New England Biolabs, Beverly, MA).

CBD and PTD4*GBA* PCR products were purified using QIAquick® PCR Purification Kits (Qiagen, Mississauga, ON) and T/A ligated into pGEM®-T Easy Vector (Promega, Madison, WI) according to the manufacturer's protocol. Ligation products (2 μl) were used to transform 40 μl of electrocompetent XL1 blue *Escherichia coli* cells using 0.2 cm Gene Pulser® cuvettes and a Gene Pulser™ electroporation machine (BioRad, Hercules, CA) set at 1.5 kV, 50 μFD capacitance, and 200 Ω resistance. SOC medium (2% (w/v) tryptone, 0.5% (w/v) yeast extract (Becton-Dickinson (BD), Oakville, ON), 10 mM NaCl, 2.5 mM KCl, 10 mM $MgCl_2$, 20 mM glucose, pH 7.0) was used to rescue cells. Cells were plated on low salt Luria-Bertani broth (1% (w/v) tryptone, 0.5% (w/v) yeast extract, 0.1 M NaCl, pH 7.5, 1.5 % (w/v) agar) containing 0.2 mM isopropyl-beta-D-thiogalactopyranoside (IPTG), 0.05 mg/ml 5-bromo-4-chloro-3-indolyl-beta-D-galactopyranoside (X-gal) (Invitrogen), and 0.12 mg/ml ampicillin (Sigma-Aldrich Canada, Oakville, ON), and incubated at 37°C for 16–18 hrs. Blue-white screening was used to identify transformants. White colonies were screened by colony PCR using 1x

PCR buffer, 3 mM $MgCl_2$, 0.2 mM dNTPs, 5 U Taq DNA Polymerase (Invitrogen), and 0.7 μM forward and reverse M13 primers (Promega). The PCR was performed as follows using both RoboCycler and GeneAmp PCR thermal cyclers: an initial denaturation at 95°C for 5 mins, 35 cycles of 95°C for 1 min, 62°C for 1 min, and 72°C for 1 min, and a final elongation at 72°C for 5 mins. PCR products of desired size, as determined by separation on a 1.5% agarose gel, indicated candidate clones for sequencing. Plasmid DNA was isolated using QIAprep® Miniprep Kit (Qiagen) according to the manufacturer's protocol. Plasmid DNA was sequenced on a LI-COR 4200-Global IR^2 sequencer (LI-COR Biotechnology) (UVic Centre for Biomedical Research DNA Sequencing Facility, Victoria, BC) with a SequiTherm EXCEL II DNA sequencing kit (Epicentre Biotechnologies, Madison, WI) using the Sanger method and vector specific (M13) labeled primers. DNA sequence data were analyzed using BioEdit sequence alignment tool (Tom Hall, Ibis Therapeutics, Carlsbad, CA).

Plasmid DNA (5μg) isolated from clones containing inserts CBD, PTD4-*GBA* or *GBA*-PTD4 was digested with the appropriate RENs for removal from pGEM®-T. The CBD insert was digested with *Eco*RI (New England Biolabs (NEB), Beverly, MA) according to the manufacturer's protocol. The PTD4*GBA* inserts were digested with both *Eco*RI and *Not*I (NEB) in a double digest reaction as follows: 15 U of both *Eco*RI and *Not*I, 1x *Eco*RI buffer, and 1x BSA (NEB) at 37°C for 3 hrs. Digestion products were run on a 1.5% (w/v) agarose gel for separation and to allow gel extraction of desired bands using a QIAquick® Gel Extraction Kit (Qiagen).

In preparation for ligation with gel-extracted CBD fragments, pPIC9K-His_6-Fxa-*GBA* was digested with *Eco*RI and dephosphorylated with calf intestinal phosphatase

(NEB) according to the supplier's recommendation. CBD inserts were ligated into linear pPIC9K-His_6-Fxa-*GBA* using a 1:3 vector to insert ratio using 1x T4 DNA ligase buffer, 2 U of T4 ligase (Invitrogen) and a 16°C 16-18 hr incubation. Similarly, PTD4*GBA* inserts were ligated into *Eco*RI/*Not*I double-digested pPIC9K.

Ligation products were used to transform XL1 blue *E. coli* cells as described previously. Transformed cells were plated on Luria-Bertani (LB) agar containing 50 µg/ml kanamycin (Invitrogen) and incubated at 37°C for 16-18 hrs. Colony PCR was used to identify insert-positive colonies as follows: 1x PCR buffer, 3 mM $MgCl_2$, 0.2 mM dNTPs, 2.5 U Taq DNA Polymerase, and 0.7 µM 5'AOX1 forward (Invitrogen) and C2 or G2 reverse primers. A GeneAmp PCR thermal cycler and the following PCR conditions were used: an initial denaturation at 94°C for 5 mins, 30 cycles of 94°C for 1 min, 54°C for 1 min, and 72°C for 1.5 mins, and a final elongation at 72°C for 7 mins. Plasmid DNA from insert positive-clones was isolated using QIAprep® Miniprep kit according to the manufacturer's protocol and sent for sequencing as described previously. DNA sequence data were analyzed using BioEdit sequence alignment tool.

Ligation of CBD into the pPIC9K-PTD4*GBA* constructs was performed as follows. *Eco*RI-digested CBD fragments were ligated into *Eco*RI-digested pPIC9K-PTD4*GBA* and transformed into XL1 blue *E. coli*, as described previously. Colonies that grew on 50 µg/ml kanamycin were screened by colony PCR following the same procedure as above using GBA specific primers (G1 and G2), a 58°C annealing temperature, and a 2 min 72°C elongation each cycle. Plasmid DNA was isolated and sequenced as described above.

2.2 Transformation of *P. pastoris* and selection and screening of transformants

Confirmed final constructs were digested (4-10 μg) with 30 U of *Sac*I, 1x NEBuffer 1 and 1x BSA (NEB) at 37°C for 5 hrs. Linear constructs (5-10 μg) were transformed into 80 μl of electrocompetent humanized *P. pastoris* strain GS115 with pGlycoSwitchM5 (obtained as a gift from Dr. Contreras, Department of Molecular Biology, Ghent University, Belgium) using 0.2 cm gap cuvettes and a Gene Pulser™ electroporation apparatus (2.5 kV, 25 μFD capacitance, and 200 Ω resistance). 1 M sorbitol and 1-2 hr incubation was used to rescue cells. Transformants were selected on histidine-deficient minimal methanol (MM) medium (1.34% (v/v) yeast nitrogen base, 4x 10^{-5} % (v/v) biotin, 0.5% (v/v) methanol, 1.5% (w/v) agar) and incubated at 30°C for 2-3 days.

Expression vector integration was determined by growth on histidine-deficient plates and direct yeast PCR. Colonies were picked, dotted on a master plate, and resuspended in 10 μl sterile water. Cells were lysed by treatment with 2 U of zymolyase (Seikagaku Corporation, Tokyo, Japan) and incubated for 2 hrs at 30°C followed by quick immersion in liquid nitrogen. Each PCR mixture contained 5 μl cell lysate, 1x PCR buffer, 2.5 mM $MgCl_2$, 0.25 mM dNTPs, 2.5 U Taq DNA Polymerase, and 0.3 μM forward and reverse primers (5'AOXI/3'AOXI, or α-secretion signal forward (Invitrogen)/3'AOXI). PCR was performed using a GeneAmp thermal cycler with a 1 min initial denaturation at 94°C, 30 cycles of 94°C for 1.5 mins, 56°C for 1.5 mins, and 72°C for 2 mins, and a final extension at 72°C for 5 mins. Clones with genomic integration, as indicated by an appropriate sized band on a 1.5% (w/v) agarose gel, were used for preliminary experiments involving protein expression. Direct yeast PCR products were sent for sequencing to confirm mutation free sequence and open reading

frame. In addition to the use of vector-specific labeled primers as described above, internal GBA-specific unlabeled primers were used on a CEQ 8000 automated sequencer (Beckman-Coulter). DNA sequence data were analyzed as described previously.

Identification of mutations in *GBA* exons 4 and 7 in constructs pPIC9K-CBD-*GBA* and pPIC9K-CBD-*GBA*-PTD4 and exons 4, 7 and 8 in construct pPIC9K-CBD-PTD4-*GBA* led to the construction of mutation free pPIC9K-*GBA*-PTD4. Restriction enzymes *Apa*I and *Psh*AI were identified as single cutters (NEBcutter V2.0, NEB) that flanked the mutations in pPIC9K-*GBA*-PTD4 (intermediate synthesized during the construction of pPIC9K-CBD-*GBA*-PTD4). Double digest reactions were performed on mutation-containing pPIC9K-*GBA*-PTD4 (6 µg), and mutation free pPICZα-*GBA* (9 µg) (provided by Dr. G. Sinclair, University of Victoria, Victoria, BC) using 25 U of *Apa*I, 12 U of *Psh*AI, 1x NEbuffer 4, 1x BSA, and a 3 hr incubation at 25°C. Digests were resolved on a 1% (w/v) agarose gel. Large pPIC9K-*GBA*-PTD4 fragments (10.2 kb) from the former digest and small *GBA* fragments (626 bp) from the latter digest were gel extracted as previously outlined. Fragments were ligated using a 1:3 vector to insert ratio and 0.5 U of T4 ligase (Invitrogen). Ligation products were transformed into chemically competent *E. coli* strain JM109 by heat shock and plated on LB containing 50 µg/ml kanamycin. Colonies were screened for presence of insert by PCR as described above and plasmid DNA from insert-positive clones was isolated and sent for sequencing to confirm removal of mutations. Plasmids were linearized with *Sac*I as before, or *Bgl*II (NEB) following the supplier's recommendations, and transformed into *P. pastoris* by electroporation. Selection by growth on histidine-deficient MM or minimal dextrose (MD) (1.34% (v/v) yeast nitrogen base, 4x 10^{-5} % (v/v) biotin, 2% (v/v) dextrose, 1.5%

(w/v) agar) and direct yeast PCR followed the same protocol described previously. Sequence analysis of direct yeast PCR products was used to confirm the error-free nature of the final construct.

2.3 Screening for Mut^S and multiple integrant clones

Growth on MD versus MM was used to identify clones with the Mut^S phenotype. Twenty five *P. pastoris* colonies, transformed with *Bgl*II digested expression vectors, that grew on MD were picked and patch plated on MM and MD. Patches that grew normally on MD plates but showed impaired growth on MM plates were designated as Mut^S.

Resistance to increasing concentrations of Geneticin® (Invitrogen) was used to select *P. pastoris* clones with multiple integrated copies of the expression vector. Several hundred colonies that grew on initial MM transformation plates were pooled, suspended in ddH_2O, and spread plated on increasing amounts of Geneticin®, from 0-1 mg/ml in 0.25 mg/ml increments. Colonies that grew on ≥0.5 mg/ml Geneticin® were considered to have two or more integrated copies of the transgene.

2.4 *P. pastoris* cell culture for recombinant GBA production

2.4.1 Small scale culture experiments

All *P. pastoris* cell culture was performed following the guidelines of the *Pichia* Expression Kit manual (Invitrogen). Baffled flasks of at least 3x the culture volume were used for all culturing. *GBA*-containing *P. pastoris* cells and vector-only negative control cells (P. pastoris transformed with pPIC9K vector not containing an insert) were inoculated in 25 ml of buffered glycerol complex medium (BMGY) (1% (w/v) yeast extract, 2% (w/v) peptone, 1.34% (v/v) yeast nitrogen base, 0.1 M sodium citrate buffer pH 5.5, 1% (v/v) glycerol, 4x 10^{-5} % (v/v) biotin). Cells were grown at 26-30^{o}C, shaking

at 250 rpm, until an optical density (OD) of 2-6 at 600 nm was reached (approximately 16-18 hrs) as determined using a Novaspec® visible wavelength spectrophotometer (Biochrom). Cells were harvested using a Sorvall RC 26 Plus centrifuge (DuPont, Newton, CT) at 3000 x g for 5 mins at room temperature (RT) (23°C). Cells were resuspended in an appropriate amount (approximately 100 ml) of buffered methanol complex medium (BMMY) (1% (w/v) yeast extract, 2% (w/v) peptone, 1.34% (v/v) yeast nitrogen base, 0.1 M sodium citrate buffer pH 5.5, 0.5% or 1% (v/v) methanol, 4x 10^{-5} % (v/v) biotin) so that an OD of 1 was obtained. Cells were cultured as before for up to 126 hrs. Cultures were supplemented with methanol to 0.5% or 1% every 24 hrs, and aliquots were taken to monitor growth, protein production, and activity at 24 hr time points. Aliquots were centrifuged at 16,000 x g for 5 mins in a Biofuge Pico microcentrifuge (Heraeus Instruments). The supernatant and pellet were separated and stored at -80°C for future analysis by sodium dodecyl sulphate polyacrylamide gel electrophoresis (SDS-PAGE) and activity assay.

2.4.2 Large scale culture experiments

Large scale expression was performed for both Mut^+ and Mut^S clones. Mut^+ large scale expression was similar to that of small scale expression (described above). A small volume (approximately 200 µl) of initial overnight 25 ml BMGY cultures was inoculated in 500 ml of BMGY media and grown overnight as described above to an OD of 2-6. Cells were harvested as outlined previously and transferred to enough BMMY media (approximately 1 litre) so that a starting OD of 1 was obtained. Induction was maintained by addition of methanol to 0.5% or 1% every 24 hrs and aliquots were taken at 24 hr time points for future analysis. Medium was harvested by centrifugation at 3000 x g for 7 mins

at 4°C after 48-72 hrs of induction. Mut^S clones were initially inoculated in 25 ml BMGY and scaled up to 500 ml BMGY as per above. Upon reaching an OD of 2-6, cells were harvested and resuspended in 1/5 the volume of BMMY. Methanol was added to 1% and aliquots were taken every 24 hrs. Medium was harvested as described above between 48-72 hrs post induction.

Cell pellets from the 1 ml aliquots taken at 24 hr time points during induction were resuspended in yeast breaking buffer (50 mM sodium phosphate (monobasic) pH 7.4, 1 mM PMSF (phenylmethylsulfonyl fluoride, a serine protease inhibitor), 1 mM EDTA, and 5% glycerol) to an OD of 50-100 to lyse cells. An equal volume of 0.5 mm acid-washed glass beads was added and samples underwent 8 cycles of vortexing for 30 secs followed by incubation on ice for 30 secs. The cell homogenate was centrifuged at 4°C at 16,000 x g for 10 mins, and the supernatant was kept for analysis by SDS-PAGE.

2.5 Reverse transcription PCR

Total RNA was extracted from cell pellets (containing approximately 2.5 x 10^7 cells) harvested at 24-72 hrs post induction using an RNeasy® Mini Kit (Qiagen). RNA extraction was performed according to the manufacturer's protocol with an off-column DNase digestion performed as follows: 1 µg RNA and 1 ul RNase free DNase (Qiagen) were incubated in 1x PCR Reaction Buffer (Invitrogen) with 5 mM $MgCl_2$ at RT for 20 mins. Reactions were stopped by heating to 65°C for 5 mins. First-strand cDNA synthesis was performed using an oligo dT primer and SuperScript® II RNase Reverse Transcriptase (Invitrogen) according to the manufacturer's protocol. The resulting cDNA was used as template in PCR: 2 µl cDNA, 1x PCR Reaction Buffer, 1.5 mM $MgCl_2$, 0.25 µM dNTPs, 0.5 µM of each primer (G1/G2 and α-secretion signal forward/C2,) and 2.5 U Taq DNA

Polymerase. Amplification was performed using a GeneAmp PCR thermal cycler with an initial denaturation of 94^{o}C for 5 mins, 35 cycles of 94^{o}C for 1 min, 58^{o}C for 1 min, 72^{o}C for 1 min, and a final elongation at 72^{o}C for 10 mins. Successful amplification, determined by electrophoresis on 1.5% (w/v) agarose gel, confirmed the presence of *GBA* transcript.

2.6 Enzyme activity assays

2.6.1 4MUGP artificial substrate assay

β-glucosidase activity in culture media and purified enzyme samples was assayed using the fluorometric 4-methyl-umbelliferyl-β-D-glycopyranoside (4MUGP) substrate (Sigma-Aldrich Canada). Ten µl of enzyme sample was added to 3.5 mM 4MUGP, 0.03 M citrate buffer pH 5.5, 0.1% (w/v) sodium taurocholate and incubated at 37°C for 30 mins. Reactions were stopped by addition of 0.2 M glycine buffer (pH 10.5) and fluorescence was assayed using a Sequoia-Turner Model 450 Digital fluorometer (Turner Designs, Sunnyvale, CA).

2.6.2 Natural substrate assay

To test for GBA activity in culture media and post-purification elutions, a natural glucocerebroside substrate activity assay was used. Assays were performed based on the following protocol (Choy and Davidson, 1980): 10-40 µl of enzyme sample were added to 1 mg/ml C_8-glucosylceramide (Avanti Polar Lipids Inc., Alabaster, AL) in 0.04 M sodium citrate buffer pH 5.5, 0.8% sodium taurocholate, and 0.1% Triton X-100^{TM}. Reaction mixtures were incubated for 4-6 hrs shaking at 37°C. Reactions were stopped by boiling for 5 mins, followed by centrifugation for 15 mins at 16,000 x g at 4°C to pellet any precipitated components. Glucose released by this reaction was measured by mixing the reaction supernatant with 10 volumes of glucose HK reagent (Sigma-Aldrich

Canada) and incubating for 10 mins at 37°C. This reaction couples hexokinase cleavage of glucose to NADH production, which is measured at 340 nm. The increase in absorbance at 340 nm is directly proportional to the glucose concentration. A UV spectrophotometer (Beckman Coulter™, DU® 530) was used to measure absorbance. Net absorbance was determined by subtraction of absorbance values due to endogenous glucose present in enzyme samples. Nmols of glucose released were calculated by comparison to a glucose standard curve (0-80 nmol), and relative and specific GBA activities were determined. All protein concentrations were determined using BioRad Protein Assay Dye Reagent (BioRad, Hurcules) and a BSA standard curve (0-2.0 mg/ml).

2.7 SDS-PAGE protein analysis

SDS-PAGE was performed using a combined gel consisting of a 10% (v/v) tris-glycine resolving gel and 4% (v/v) tris-glycine stacking gel. Samples were prepared with 3x SDS sample buffer (NEB), mixed with 42 mM dithiothreitol (DTT). Samples were boiled for 5 mins, pH adjusted with NaOH, and centrifuged at 16,000 x g for 5 mins. Gels were run on a Mini-Protean® Tetra Cell electrophoresis unit (BioRad). A Precision Plus dual colour marker (BioRad) or prestained colour marker (NEB) was used to estimate the molecular mass of separated proteins.

2.7.1 Silver stain analysis

Gels containing proteins separated by SDS-PAGE were microwaved for 90 secs in fixative (50% (v/v) methanol, 12% (v/v) acetic acid, 0.1% (v/v) formaldehyde), followed by a 90 sec microwave in 50% (v/v) ethanol. Gels were then microwaved for a further 90 secs in a pretreatment solution (0.02% (w/v) sodium thiosulfate pentahydrate), and rinsed in ddH_2O for 90 secs at RT. Staining was achieved in 2 mg/ml silver nitrate in 0.075%

(v/v) formaldehyde by microwaving twice for 40 secs, with 20 secs of shaking at RT between microwaving. A 90 sec rinse in ddH_2O preceded protein band resolution in developer solution (60 mg/ml sodium carbonate, 0.05% (v/v) formaldehyde, 0.002% (w/v) sodium thiosulfate pentahydrate). Gels were clarified in 5% (v/v) acetic acid and stopped by addition of 50% (v/v) methanol.

2.7.2 Immunoblotting

Proteins separated by SDS-PAGE were transferred to BioTrace™ polyvinylidene fluoride (PVDF) transfer membranes (Pall Corporation) at 10V for 14-17 hrs in 10% (v/v) methanol transfer buffer (25 mM tris-HCl, 0.2 M glycine) using a Mini Trans-Blot® Cell apparatus (Biorad). The following steps were performed at RT with gentle shaking post transfer. PVDF membranes were rinsed in phosphate buffered saline and 0.2% (v/v) Tween 20 (PBST), blocked with 5% (w/v) skim milk for 1 hr, incubated with primary anti-human GBA monoclonal antibody (mAb) H00002629-M01 (Abnova Corporation, Taipei City, Taiwan) at a 1:1000 dilution for 1-2 hrs, washed with PBST 3x 10 mins, incubated with 2° goat anti-mouse horseradish peroxidase conjugated secondary antibody (Pierce, Rockford, IL) at a 1:1000 dilution in blocking solution for 1 hr and washed with PBST 3x 10 mins. Blotted membranes were reacted with SuperSignal® West Dura extended duration substrate (Pierce) for 5 mins before being exposed to CL-X Posure™ film (Pierce) for various lengths of time and visualized by autoluminography. Relative band intensity was determined using Image J software.

2.8 Purification of GBA-PTD4

2.8.1 Hydrophobic interaction chromatography

Crude *P. pastoris* medium was centrifuged at 8000 x g for 20 mins at 4°C in a Sorvall® RC 26 Plus centrifuge and either concentrated (Mut^+) 2-10 fold or used directly (Mut^S) in purification. Concentration was performed using an amicon stirred ultrafiltration cell (model 8200) and NMWL 50,000 ultrafiltration membranes (Millipore Corporation, Billerica, MA). Hydrophobicity of proteins in medium was induced by addition of ammonium sulphate to 1.2-1.4 M, followed by gentle agitation and incubation on ice for 20 mins. Medium was centrifuged at 8000 x g for 20-30 mins at 4°C and the supernatant was degassed through a 0.45 μm membrane (Pall Gelman Laboratories, Ann Arbor, MI). All buffers and solutions were degassed prior to use and, along with FPLC equipment, were kept on ice throughout the purification procedure. Using a Pharmacia LKB P-500 pump (Pharmacia), or a AKTA prime FPLC system (Amersham Biosciences), samples were loaded onto a 5 ml HiTrap™ Phenyl HP column (GE Healthcare, Uppsala, Sweden) at 0.5-3 ml/min. Columns had been previously equilibrated with buffer A (1.2-1.45 M $(NH_4)_2SO_4$, 50 mM sodium-citrate, 0.1 M NaCl, pH 5.5). Following sample loading, a desalting gradient was established from 100% buffer A to 100% buffer B (50 mM sodium-citrate, 0.1 M NaCl, pH 5.5) over 80-100 ml at 0.5-1 ml/min. At a flow rate of 1-2 ml/min 40-50 ml of water was passed over the column before a 40-60 ml linear gradient of 0-3% cholic acid was started. Column elutions were collected on ice in 1-10 ml fractions and analyzed by activity assay and SDS-PAGE. Samples determined to contain GBA were supplemented with 5 mM DTT or β-mercaptoethanol and frozen for further analysis or used promptly for subsequent

purification. Purification yield was calculated by comparison of total GBA activity or total GBA amount in post-purification samples to pre-purification samples.

2.8.2 Gel filtration chromatography

Partially purified GBA samples from HIC were pooled, concentrated and diafiltrated into buffer B for a ~15 fold volume decrease using Amicon® Ultra centrifugal filter units with 50,000 MWCO pore size (Millipore, Cork, Ireland) and a Sorvall® RC 26 Plus (Se-13 rotor) centrifuge set at 7000 x g. Buffers, samples and equipment were kept on ice throughout the purification procedure. Approximately 250 µl of concentrated GBA sample was injected onto a Superose 12 10 mm/300 mm gel filtration column (Pharmacia), attached to a Pharmacia LKB P-500 pump, equilibrated with degassed 50% (v/v) ethylene glycol with 0.1 M citrate and 0.1 M NaCl at pH 5.5. Application of ethylene glycol/citrate buffer was resumed at a flow rate of 0.1-0.15 ml/min and one void volume (V_o= 6ml) was allowed to pass through the column before fraction collection was started. Fractions of 0.6 ml were collected for a total of 25 ml. Eluted fractions were analyzed for protein concentration on a UV spectrophotometer (Beckman Coulter™, DU® 530) and activity using the 4MUGP assay. Purification yield was calculated by comparison of total GBA amount in purified samples to pre-purification samples.

Chapter 3 – Results

3.1 Construction of expression vectors

PCR was used to amplify the 1.5 kb human *GBA* cDNA sequence, with and without flanking PTD4, and the 370 bp sequence for CBD that were used in our expression vectors. PCR-amplified inserts were cloned into pPIC9K, after bacterial propagation using pGEM®-T vectors, for expression in *P. pastoris*. Figure 3.1 shows bands for pPIC9K (9.3 kb), GBA (1.5 kb), and CBD (370 bp) in a 1% (w/v) agarose gel after digestion of the following DNA constructs with *Eco*RI and *Not*I: pPIC9K-CBD-PTD4-*GBA*, pPIC9K-CBD-*GBA*-PTD4, pPIC9K-*GBA*-PTD4, and pPIC9K only. DNA sequence analysis confirmed the presence, orientation, and correct open reading frame of desired insert components.

3.2 Transformation of *P. pastoris* with *GBA*-containing pPIC9K expression vectors

P. pastoris clones transformed with *GBA* expression vectors and pPIC9K vector only were selected for genomic integration by growth on histidine deficient plates and screened for the presence of *GBA* inserts by direct yeast PCR. Vector- and insert-specific primers were successful in identifying clones that contained *GBA* sequences (Figure 3.2). Figure 3.2a shows amplification, using insert-specific primers, of the GBA portion of integrated pPIC9K-CBD-*GBA* (1.5 kb) (indicated by arrow). Figure 3.2b shows DNA bands, amplified using vector-specific primers (α-secretion signal forward and 3'AOXI), representing constructs pPIC9K-CBD-PTD-*GBA*, and pPIC9K-CBD-*GBA*-PTD (2.1 kb) (indicated by arrow). The approximate 1.7 kb band seen (indicated by a star) represents amplification of an α-mannosidase gene, inherent to the humanized *P. pastoris* strain.

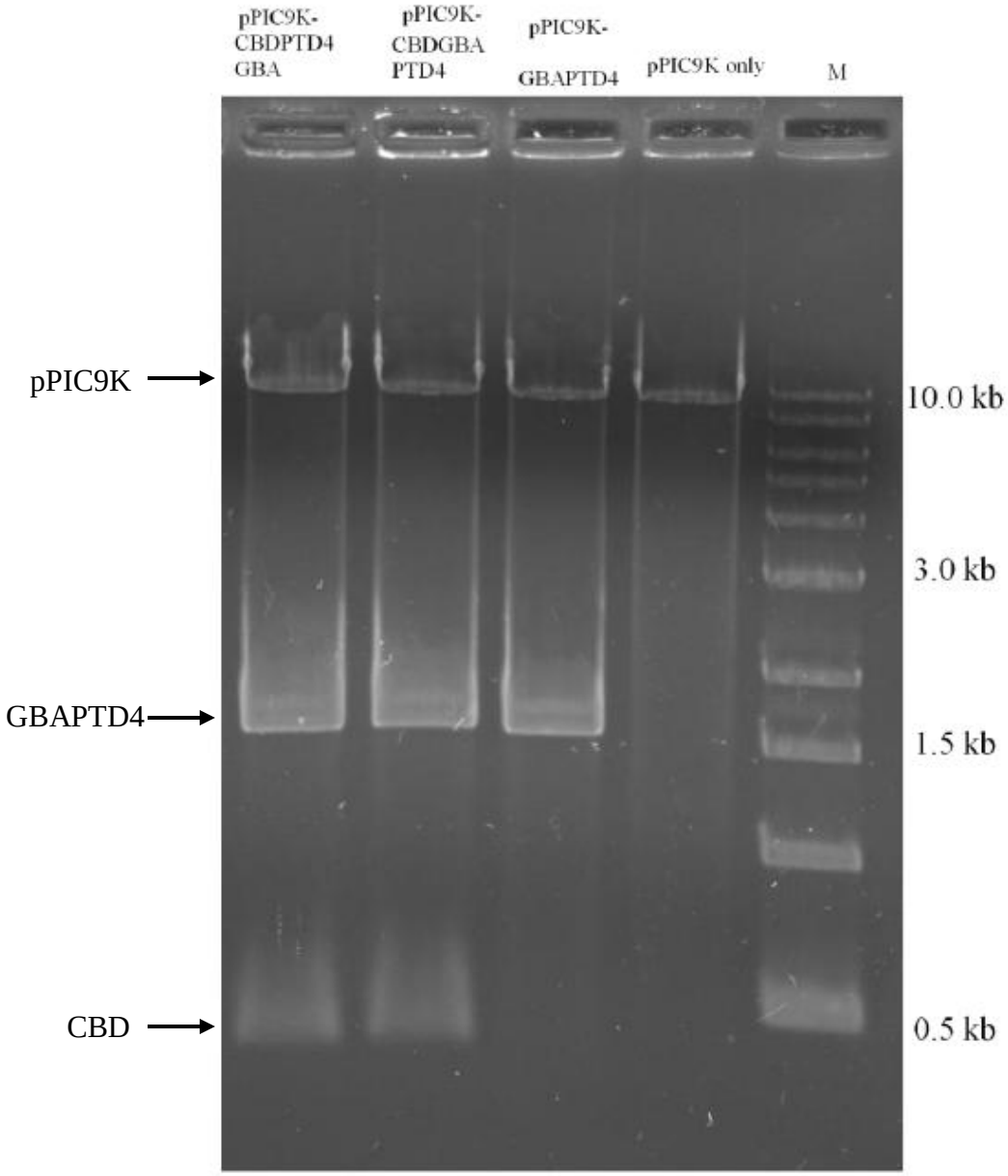

Figure 3.1 Agarose gel of *Eco*RI and *Not*I digested pPIC9K expression vectors created for GBA expression studies. Indicated by arrows are the pPIC9K vector (9.3 kb), GBA with fused PTD4 (1.5 kb), and CBD (370 bp). A 1 kb DNA standard (NEB) is shown in lane M.

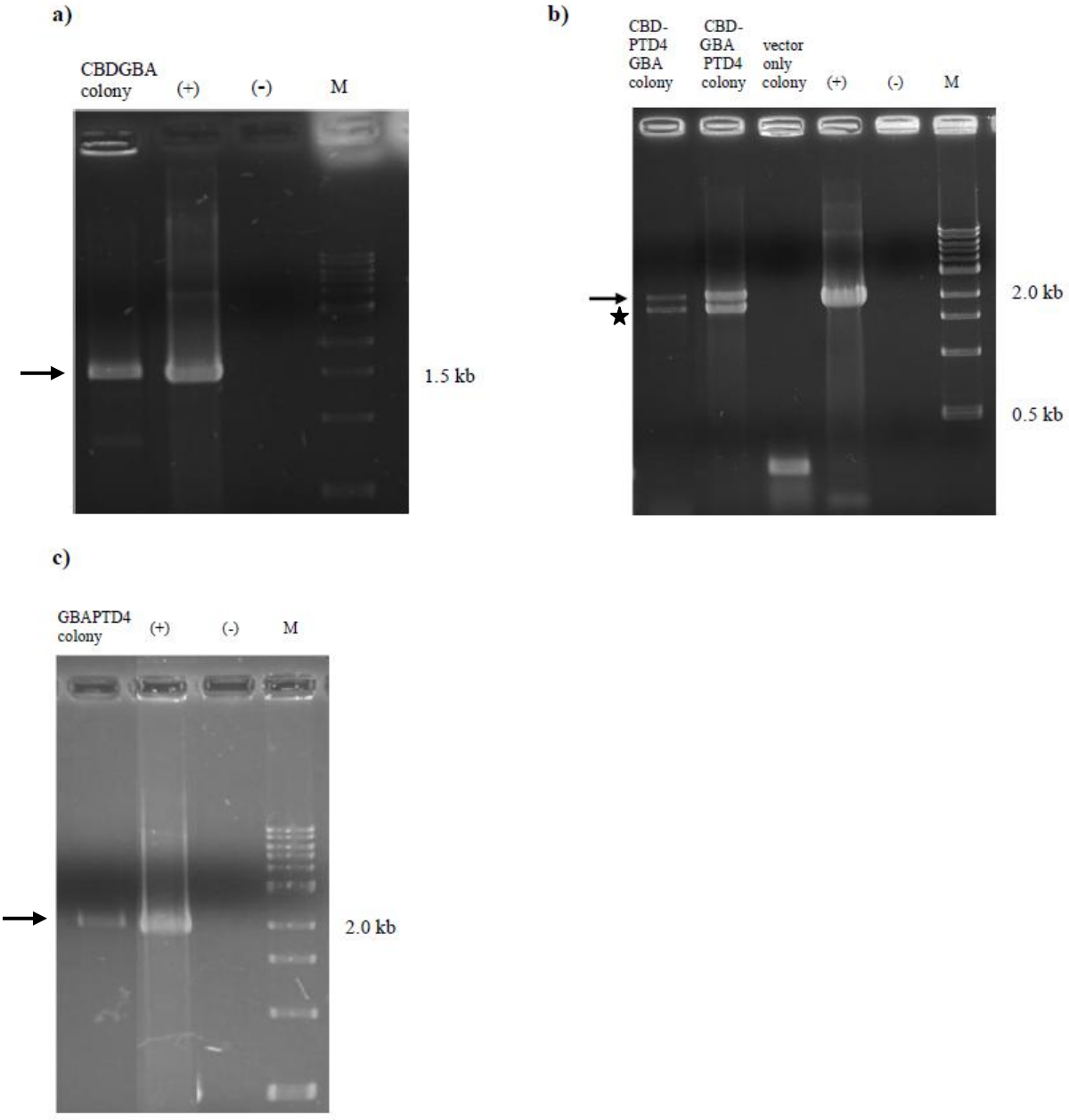

Figure 3.2 Agarose gels of direct yeast PCR products confirming integration of *GBA*-containing pPIC9K expression vectors into *P. pastoris* genome. Genomic DNA from *P. pastoris* transformed with **a)** pPIC9K-CBD-*GBA*, amplified with *GBA*-specific primers, **b)** pPIC9K-CBD-PTD4-*GBA* and pPIC9K-CBD-*GBA*-PTD4, amplified with vector-specific α-secretion signal and 3'AOXI primers, and **c)** pPIC9K-*GBA*-PTD4, amplified with vector-specific 5' and 3' AOXI primers. Arrows indicate GBA-sized bands of expected sizes. Star indicates unexpected amplification of an α-mannosidase gene. Plasmid DNA was used as a positive PCR control (+). Water negative PCR controls (-) are also shown. M denotes a 1 kb DNA standard (NEB).

Figure 3.2c shows amplification, using 5' and 3' AOXI primers, of construct *GBA*-PTD (2.0 kb) (indicated by arrow).

Sequencing of amplicons from direct yeast PCR led to identification of mutations in CBD-*GBA*, CBD-PTD4-*GBA*, and CBD-*GBA*-PTD4 constructs. The same mutations, in exons 4 and 7, were present in all three constructs in the *GBA* cDNA. The exon 4 mutation consisted of a G-to-A change resulting in an alanine-to-threonine switch at amino acid position 84. The exon 7 mutation resulted from a T-to-G change resulting in a leucine-to-arginine switch at amino acid position 264. An additional mutation in exon 8 was present in the CBD-PTD4-*GBA* construct which consisted of a T-to-C change resulting in a methionine-to-threonine alteration at amino acid position 361. Sequence analysis of *P. pastoris*-integrated pPIC9K-*GBA*-PTD4 confirmed that it was error free.

3.3 Selection of Mut^S and multiple integrant *P. pastoris* clones

3.3.1 Selecting a clone with the Mut^S phenotype

The methanol utilization status of *P. pastoris* clones (Mut^+ and Mut^S) can be an important factor in heterologous protein production. Optimal expression in Mut^+ versus Mut^S is protein specific; therefore, we investigated GBA expression in both Mut^+ and Mut^S clones. Production of Mut^S clones can be facilitated by digestion of the pPIC9K expression vector with *Bgl*II prior to transformation; this encourages homologous recombination at the AOXI site, causing disruption of the *AOXI* gene. Both Mut^+ and Mut^S clones were screened by phenotypic growth comparison on glucose and methanol. Figure 3.3 shows 25 colonies patch-plated on minimal media plates containing

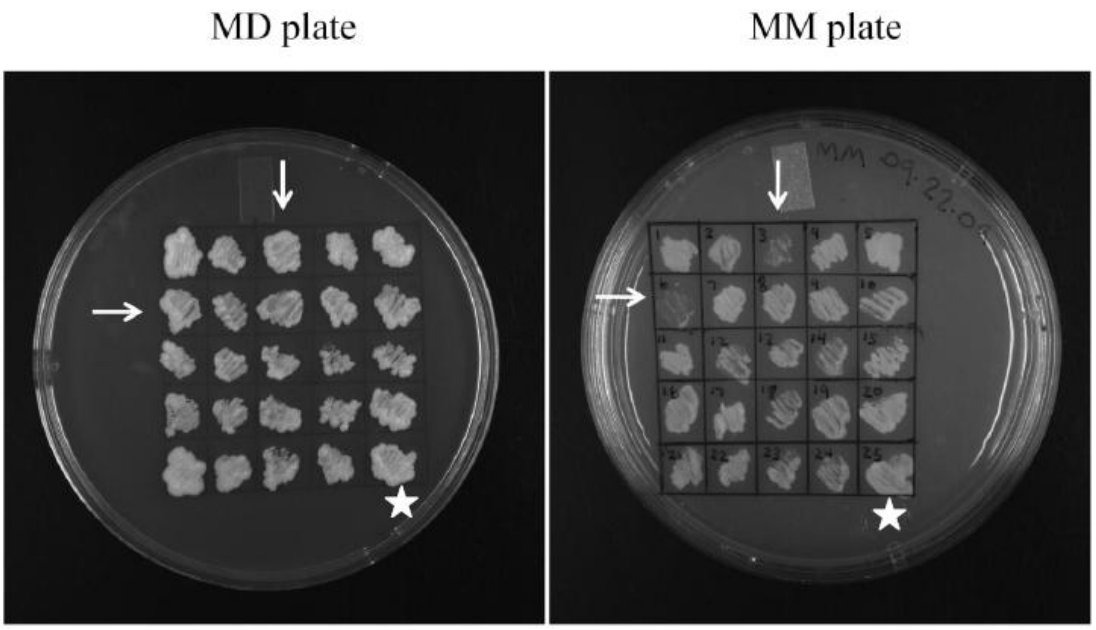

Figure 3.3 Screening for methanol utilization slow (Mut^S) clones by comparing growth on glucose (MD plate), and methanol (MM plate). Clones 3 and 6 (indicated by white arrows) show impaired growth on methanol compared to glucose and are considered Mut^S clones. Clone 25 (indicated by white star) is an example of a clone that grew well on both glucose and methanol and is considered a methanol utilization plus (Mut^+) clone. Indicated clones 3 and 25 were selected for expression studies.

either glucose (MD) or methanol (MM). Clones 3 and 6 (indicated by arrows) grew well on glucose but show poor growth on methanol (Figure 3.3) and thus display the slow methanol utilization phenotype. Clone 3 was selected for expression studies. Clone 25 (indicated by a star) grew well on both glucose and methanol thus displaying Mut^+ growth characteristics (Figure 3.3) and was chosen for use in expression studies.

3.3.2 Selecting a clone with multiple integrated copies of pPIC9K-*GBA*-PTD4

The pPIC9K vector has the ability to generate transgenic yeast with multiple integrated copies of the expression vector for increased expression potential. Homologous recombination between the expression vector and the host's genome occurs at a targeted site and on occasion multiple-targeted integration events will occur. We screened for multiple copy integrants to use in our expression studies. *P. pastoris* clones with multiple copies of the pPIC9K expression vector will have increased resistance to Geneticin® due to multiple copies of this antibiotic resistance gene, which is present in the pPIC9K vector. Therefore, growth on increasing concentrations of Geneticin® can be used to select for clones with multiple integration events. Growth on approximately 0.25 mg/ml Geneticin® suggests 1 integrated copy of the expression vector, while growth on 0.5 mg/ml indicates 1-2 copies. Growth on Geneticin® concentrations up to 4.0 mg/ml is indicative of clones with 7-12 integrated copies of the transgene (pPIC9K manual, Invitrogen). Clone 25 grew well on 0.75 mg/ml Geneticin® (not shown) and was suspected to be a >2x integrant. This was the Mut^+ clone used in expression studies. Selected Mut^S clone 3 was also grown on increasing amounts of Geneticin®. Inability to grow on Geneticin concentrations above 0.25 mg/ml (not shown) indicated the likelihood that this clone contained one copy of integrated pPIC9K-*GBA*-PTD4.

3.4 Protein Expression

3.4.1 Initial attempts to detect expression of mutant GBA

Preliminary expression of CBD-*GBA*, CBD-PTD4-*GBA*, and CBD-*GBA*-PTD4 in *P. pastoris* was performed in small-scale cultures including a vector-only negative control to determine the optimal time-point post methanol induction for expression. GBA was not detectable in the medium from these small cultures so expression was scaled up. Recombinant protein production was assessed by activity assay and SDS-PAGE silver stain and immunoblotting. Detection of expression with the artificial substrate, 4MUGP, was futile due to the high levels of background fluorescence caused by non-specific β-glucosidase activity endogenous to *P. pastoris*. Figure 3.4a shows an insignificant difference in fluorescence between medium from GBA transformed cells and vector-only transformed cells. Medium was concentrated and a natural lipid substrate assay was used. Activity was not detected with this assay; levels of glucose released in the reaction did not exceed background levels (included in Figure 3.9). Silver staining of SDS-PAGE-separated proteins showed subtle differences in protein band patterns between media from GBA-containing yeast and vector-only clones; however no obvious band representing GBA was present (Figure 3.4b). Bands in an anti-GBA immunoblot were not visible when crude or several-fold-concentrated induction medium was analyzed (included in Figure 3.7).

Therefore, reverse transcription (RT) PCR was used to look for the presence of GBA mRNA in *Pichia* transformants to assess whether transcription was occurring. Figure 3.5 shows bands in a 1.5% (w/v) agarose gel of reverse-transcribed mRNA

a)

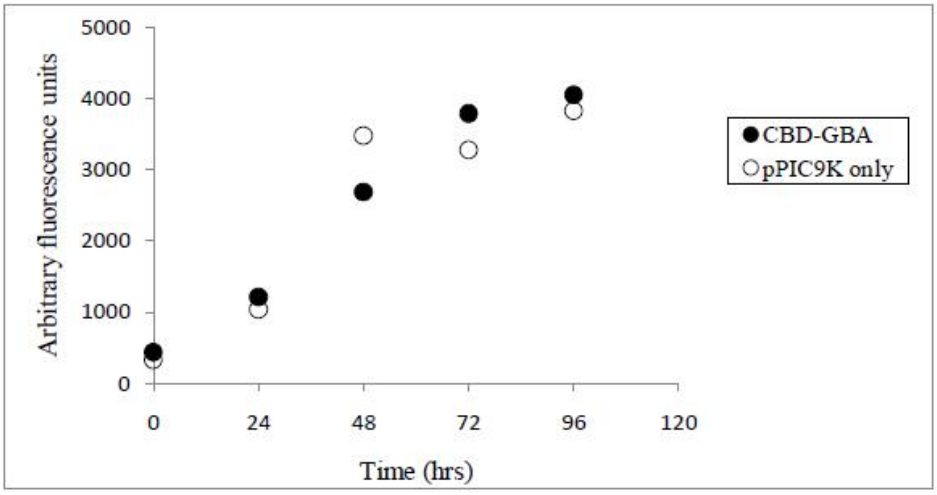

b)

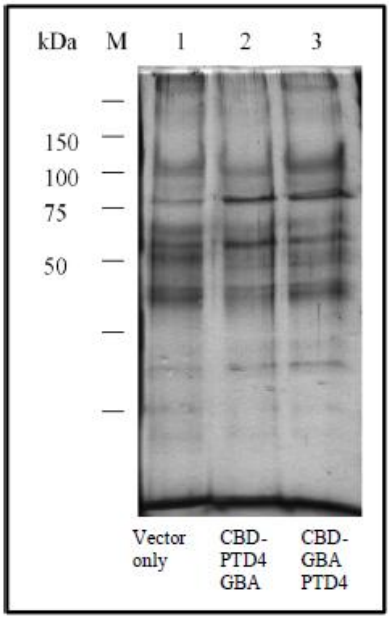

Figure 3.4 No detectable production of mutant GBA from *P. pastoris* by a) 4MUGP activity assay or b) SDS-PAGE silver stain analysis. **a)** Arbitrary fluorescence units from CBD-GBA (●) and vector-only (○) media harvested at 24 hr time points during methanol induction assayed with 4MUGP substrate. Fluorescence was measured using a Sequoia-Turner Model 450 fluorometer. **b)** Silver stain of SDS-PAGE separated proteins from vector-only (lane 1), CBD-PTD4-GBA (lane 2), and CBD-GBA-PTD4 (lane 3) media harvested 48 hrs after induction. M denotes a protein standard (BioRad, 161-0374).

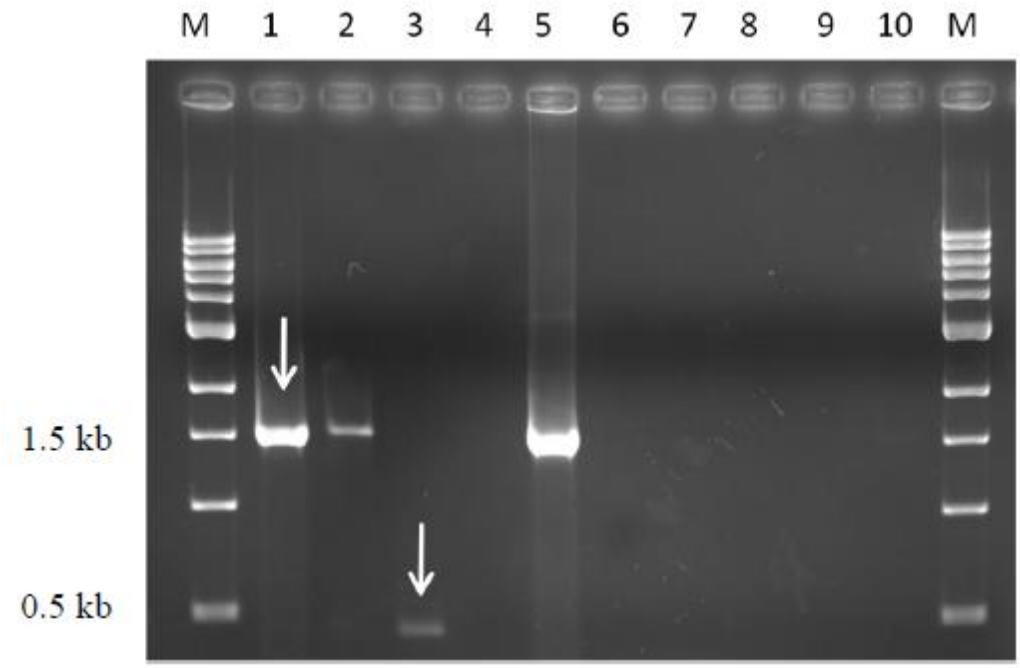

Figure 3.5 Agarose gel of reverse transcription PCR amplicons showing presence of insert-specific mRNA in CBD-*GBA* (lane1), CBD-PTD4-*GBA* (lane 2), and CBD-*GBA*-PTD4 (lane 3) transformed *P. pastoris*. Lanes 1 and 2 show amplification of the GBA portion of mRNA using GBA-specific primers (indicated by arrow). Lane 3 shows presence of the CBD portion of mRNA using CBD- and vector-specific primers (indicated by arrow). Lane 4 represents a negative control, containing cDNA from pPIC9K only transformed cells. Lane 5 shows amplification of positive plasmid DNA control. Lanes 6-9 contain non-reverse transcribed RNA from the corresponding samples in lanes 1-4. Lane 10 contains negative PCR water control. M denotes DNA standard 1 kb marker (NEB).

amplified with insert- and vector-specific primers. The 1.5 kb (lanes 1 and 2) and 439 bp (lane 3) bands represent amplification of GBA mRNA from CBD-GBA and CBD-PTD4-GBA samples and CBD mRNA from a CBD-GBA-PTD4 sample, respectively. These RT-PCR results indicate the presence of CBD-GBA transcript and confirm transcription. No bands are present in the vector only negative control (lane 4) or in the non-reverse transcribed samples (lanes 6-9), indicating that amplification was from cDNA and not genomic DNA.

Transcription was confirmed but the presence of active enzyme in induction medium was still unclear. The *P. pastoris* cell pellet was analyzed for the presence of GBA to assess whether secretion of the GBA polypeptide was being hampered. Immunoblot analysis of cell lysate proteins showed the presence of GBA-specific bands of smaller-than-expected size (Figure 3.6a, lane 3). The expected size of human GBA with correct glycosylation is between 62 and 67 kDa (Choy and Woo, 1991; Berg-Fussman et al., 1993), with the addition of fused CBD we predict a polypeptide of approximately 85 kDa. Cell pellet samples represent a much more concentrated protein fraction compared to the same volume of medium. Upon excessive concentration (approximately 30 x) of induction media, immunoblot analysis revealed cross-reactive anti-GBA bands (Figure 3.6a-c). Figure 3.6a shows an immunoblot of medium (lanes 1-2) and cell lysate (lanes 3-4) from CBD-PTD4-GBA and pPIC9K-only cells. GBA-specific bands of various smaller-than-expected sizes were present in both medium and cell-lysate samples from this construct. Figures 3.6b and c show immunoblots of CBD-GBA and CBD-GBA-PTD4 media, respectively, concentrated approximately 30-fold, and equally concentrated pPIC9K-only medium. GBA specific bands of expected size

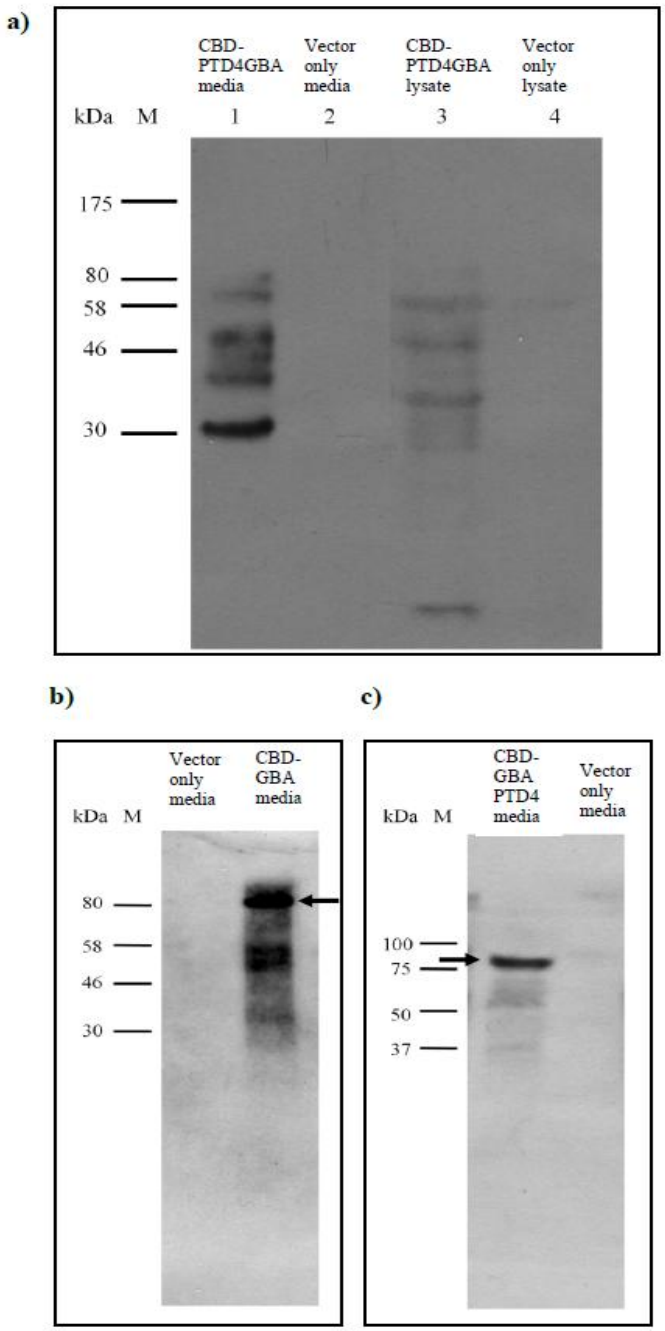

Figure 3.6 Immunoblots of GBA in a) cell lysate and a-c) induction medium. a) 30x concentrated induction medium, and cell lysates from CBD-PTD4-GBA and pPIC9K-only cultures harvested at 48 hrs post induction. b) 30x concentrated pPIC9K-only and CBD-GBA medium. c) 30x concentrated CBD-GBA-PTD4 and pPIC9K-only media. GBA-specific bands of expected size (approximately 85 kDa) (indicated by arrows) and degraded GBA bands are seen. Immunodetection was performed using an anti-human GBA mAb (Abnova, H00002629-M01). M denotes a protein standard (NEB P7707 (a and b), BioRad 161-0374(c)).

(approximately 85 kDa) (indicated by arrows) as well as smaller bands are seen. Together these results suggest low levels of secreted and sequestered mutant GBA from *P. pastoris* with undetectable activity.

3.4.2 Expression of error-free GBA

GBA-PTD4 *P. pastoris* clones were cultured for 126 hrs with aliquots taken every 24 hrs to determine the optimal time point for expression. Figures 3.7 and 3.8 show immunoblots displaying clear differences in band intensity between time points, with the most intense GBA bands (~63 kDa representing whole polypeptide; ~45 and ~35 kDa representing degraded protein) present in the 48 hr samples. These results indicate that 48 hrs post induction is optimal for GBA expression. Decreased band intensity is seen at 24 and 77 hr time points (Figure 3.7) and no GBA was detected in 102 and 126 hr samples (Figure 3.8).

To compare expression of error-free GBA-PTD4 to that of mutant (Δ84 & 264) GBA-PTD4, immunoblots of unconcentrated media were conducted. Detection with an anti-GBA mAb revealed cross-reactive bands in error-free GBA-PTD4 media, but not in mutant GBA-PTD4 medium (Figure 3.7). This confirmed increased expression of error-free GBA-PTD4 compared to mutant GBA-PTD4. No further work was carried out with mutant GBA.

Comparing expression of Mut^+ and Mut^S clones by immunoblot showed significantly more intense GBA bands (approximately 63 kDa) in Mut^S samples compared to Mut^+ samples (Figure 3.8). At each time point compared (24, 48 and 77 hrs) Mut^S samples showed more intense GBA bands than Mut^+ samples (Figure 3.8), indicating increased expression of GBA from Mut^S transformants.

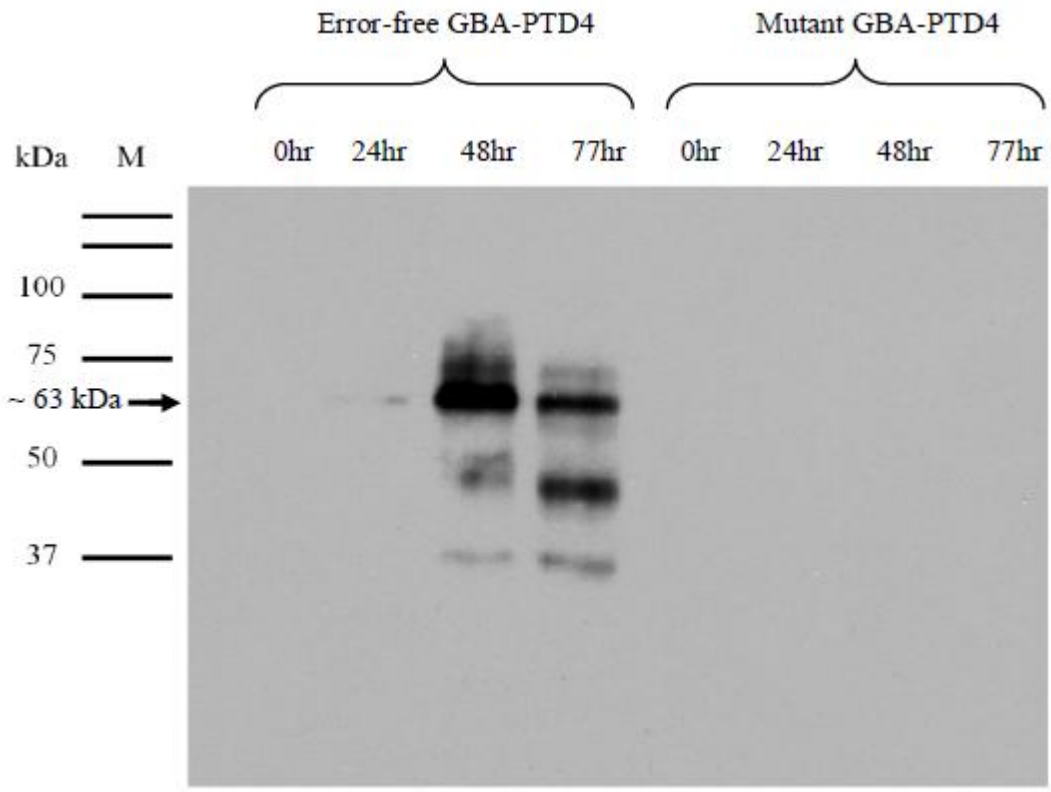

Figure 3.7 Immunoblot of error-free GBA-PTD4 and mutant GBA-PTD4 0-77 hr unconcentrated induction medium. GBA-specific bands (~63 kDa representing whole polypeptide (indicated by arrow); ~45 and ~35 kDa representing degraded protein) are visible in error-free medium at 24-77 hr time points. Immunodetection was performed using an anti-GBA mAb (Abnova, H00002629-M01). M denotes a protein standard (BioRad 161-0374).

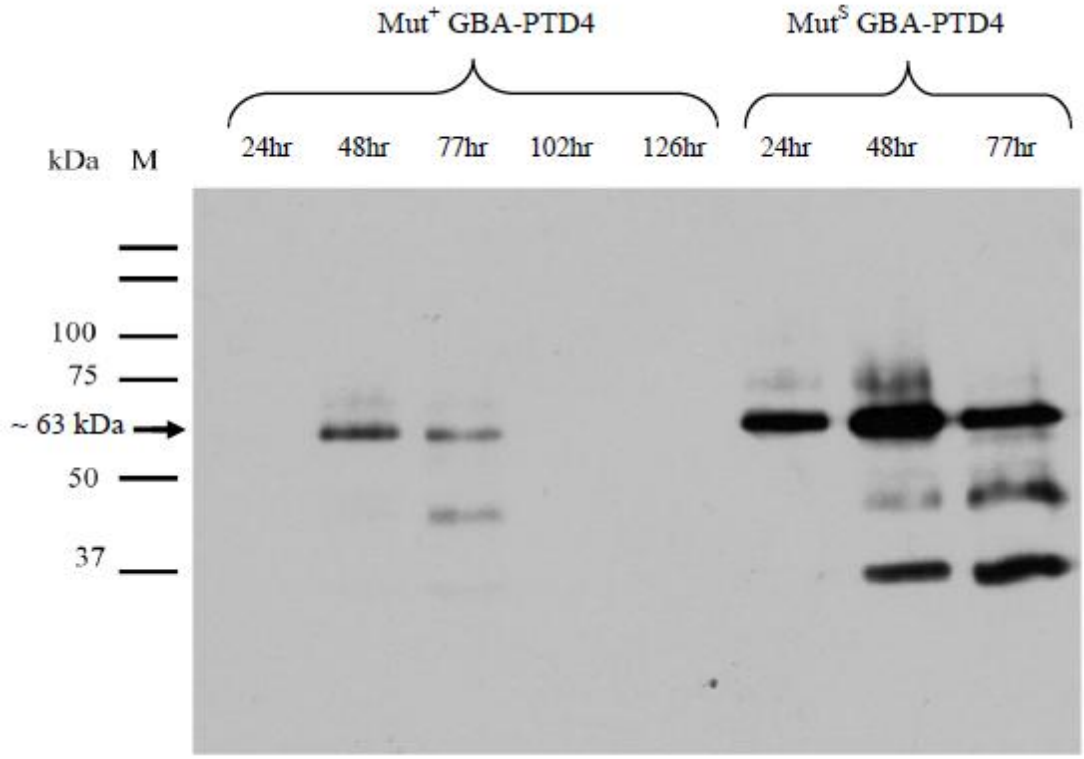

Figure 3.8 Immunoblot of Mut^+ 24-126 hr and Mut^S 24-77 hr GBA-PTD4 unconcentrated induction medium. GBA-specific bands (~63 kDa representing whole polypeptide (indicated by arrow); ~45 and ~35 kDa representing degraded protein) are more intense in Mut^S compared to Mut^+ samples at each time point. Immunodetection was performed using an anti-GBA mAb (Abnova, H00002629-M01). M denotes a protein standard (BioRad 161-0374).

Activity was detected in concentrated medium from large-scale induction of Mut^S and Mut^+ transformants (Figure 3.9). Concentration of samples by either 40% (w/v) ammonium sulphate precipitation or ultra-filtration using 50,000 MWCO centrifugal devices was necessary in order to detect activity with this assay. Figure 3.9 shows approximately 170 nmol glucose/hr/mg of GBA activity in media from Mut^S clone 3. Mut^+ clone 25 appeared to produce less than half the activity compared to the Mut^S clone (Figure 3.9). We concluded that optimal expression of active GBA from *P. pastoris* occurs at 48 hrs post induction from cells containing disrupted *AOXI* genes (Mut^S).

3.5 Purification of GBA-PTD4

3.5.1 Hydrophobic interaction chromatography

Hydrophobic interaction chromatography (HIC) was used for purification of GBA-PTD4 from *P. pastoris* induction medium. GBA is well-suited to this method due to its strong hydrophobic nature; GBA is an endogenous membrane-associated hydrophobic protein. This technique involved three principle stages: a desalting gradient, where loosely associated proteins will elute from the column; a water wash, where weak to moderate hydrophobic interactions will be disrupted; and a cholate gradient (0-3%), where strongly hydrophobic proteins will elute from the column (Reviewed by Queiroz et al., 2001). Eluted fractions from each stage were analyzed for presence of GBA, although it was expected that this highly hydrophobic protein would elute in the cholate gradient. Fractions were analyzed initially for presence of protein by absorbance readings at 280 nm and for β-glucosidase activity by 4MUGP assay. Figure 3.10a shows a number of protein peaks present in the desalting gradient, one major peak in the water wash, and several small peaks in the cholate gradient. Figure 3.10b shows two significant peaks in fluorescence, a large one in the desalting gradient and a lesser one in

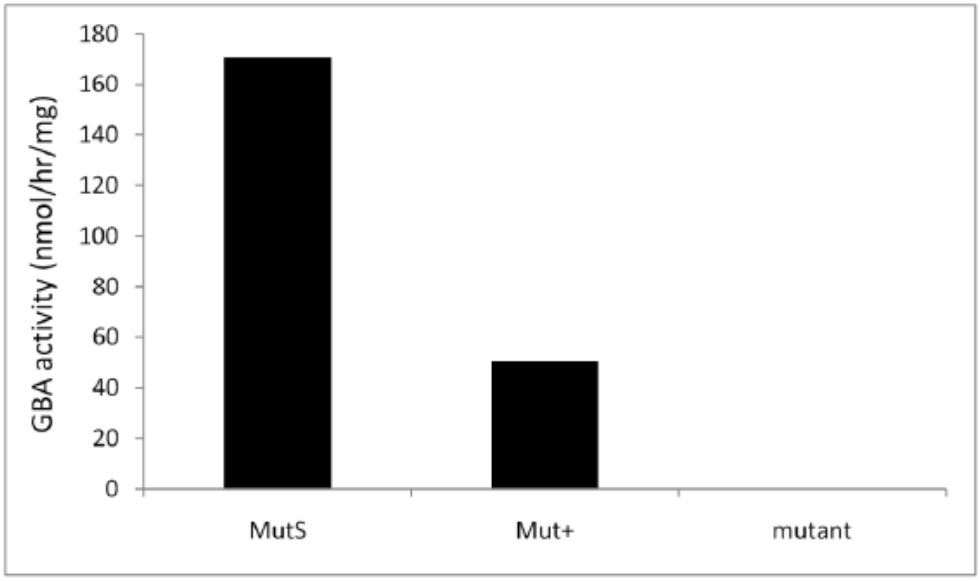

Figure 3.9 GBA activity in Mut^S and Mut^+ GBA-PTD4 and mutant GBA-PTD4 48 hr concentrated induction medium in nmol glucose/hr/mg protein determined using a natural lipid substrate assay. These data were calculated from a single trial but are representative of multiple trials assayed.

a)

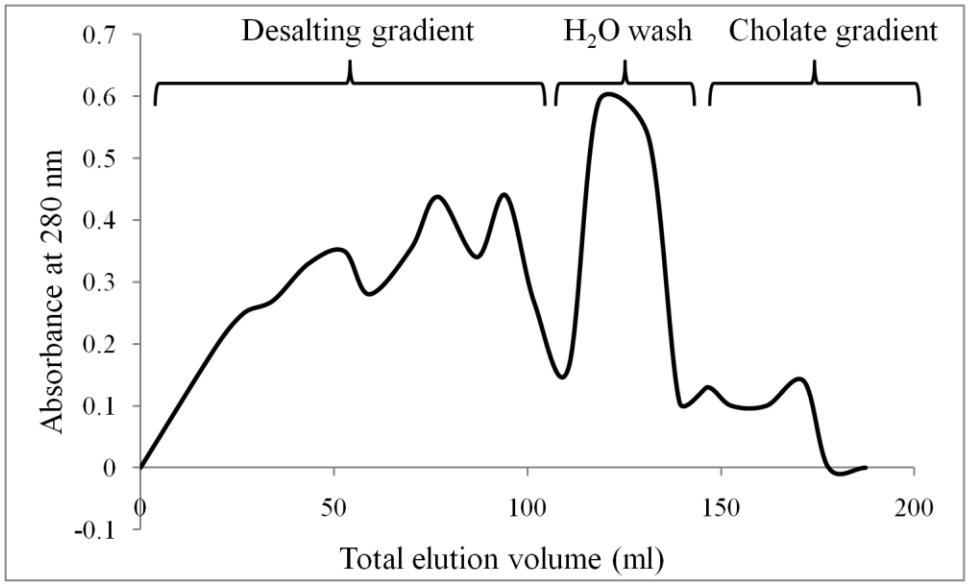

b)

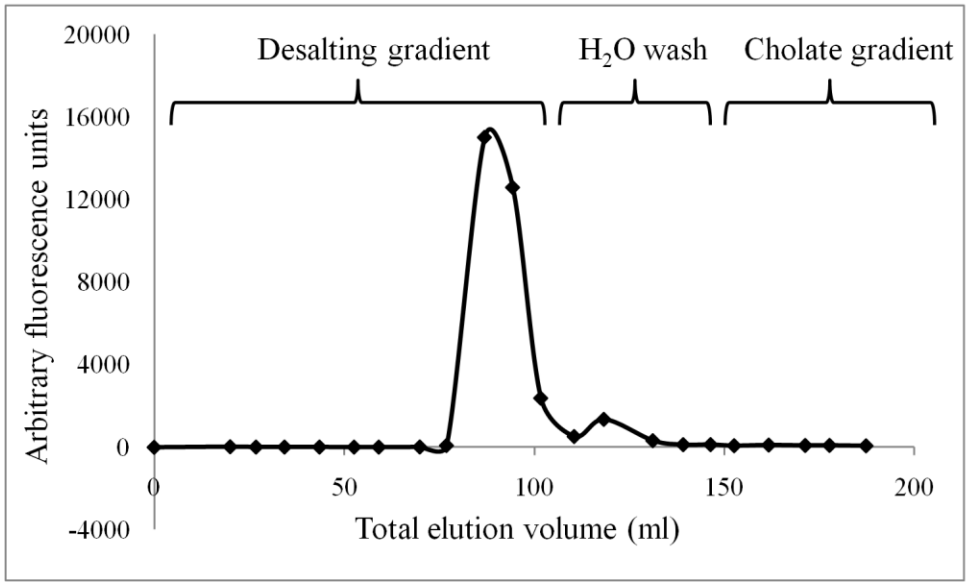

Figure 3.10 Elution profile from hydrophobic interaction chromatography of GBA-PTD4 from *P. pastoris* induction medium. **a)** Absorbance at 280 nm and **b)** fluorescence due to β-glucosidase activity generated from 4MUGP assay of fractions collected over total elution volume.

the water wash. Small AFU peaks were also present in the cholate gradient but are not visible on the plot due to their small scale relative to major peaks (Figure 3.10b). Several neighbouring fractions from principle protein and absorbance peaks were pooled, concentrated, and analyzed specifically for GBA by immunoblot and natural substrate activity assay. Samples were also analyzed by silver stain to observe the total number of protein bands in various fractions as an indication of purity. The immunoblot in Figure 3.11a shows no detectable GBA in the desalting gradient (lane 1), while GBA is detected in the water wash and cholate gradient samples (lanes 2-7), with the majority being present in the water wash (lanes 3-4). Similarly, GBA activity data shows that the majority of active GBA is present in water-wash samples, less active GBA is in cholate gradient samples, and the lowest levels of GBA activity are present in desalting gradient fractions (Figure 3.12). Silver stain analysis shows that the GBA present in water-wash samples is co-purified with multiple other proteins (Figure 3.11b, lanes 3-5); further purification is needed if homogenous GBA is desired. However, faint GBA bands appear to be the only visible proteins in silver-stained cholate gradient samples (lanes 6-7), indicating successful purification.

Purification yield was calculated based on total activity (nmols/hr) from all HIC fractions with measurable activity compared to the pre-purification medium. Based on these calculations, approximately 10% of GBA was recovered after purification on HIC (Table 3.1a). This value indicates either that a substantial amount of GBA was lost during purification, or that a significant loss in GBA activity occurred during or after purification. To determine the cause for this low apparent recovery, we used

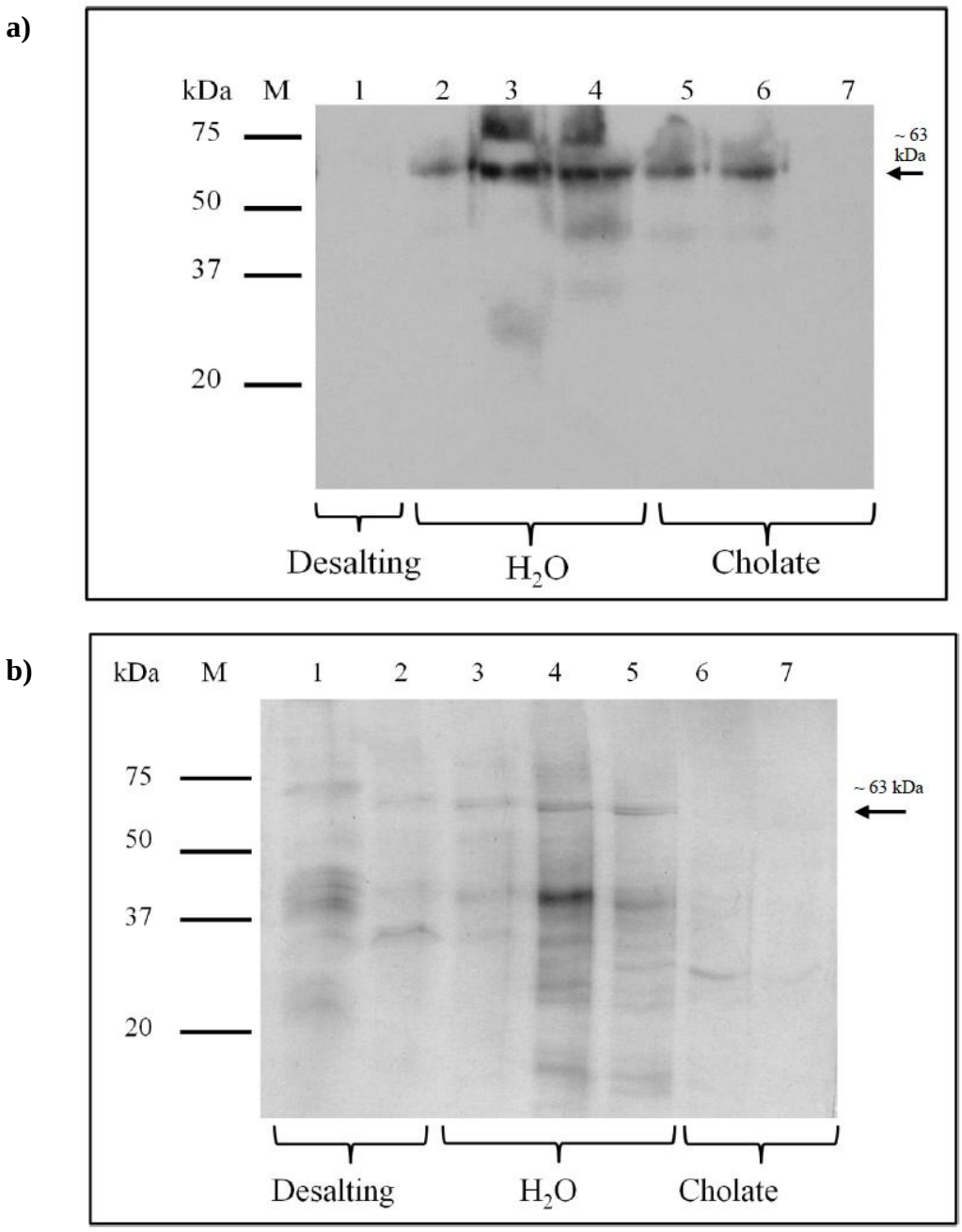

Figure 3.11 Purification of GBA-PTD4 from *P. pastoris* induction medium by hydrophobic interaction chromatography. **a)** Immunoblot of peak fractions, pooled and concentrated, from desalting gradient, water wash, and cholate gradient. GBA-specific bands (~63 kDa) are seen in the water wash and initial cholate gradient fractions (lanes 2-7), while no bands are seen in the desalting gradient fraction (lane 1). Immunodetection was performed using an anti-GBA mAb (Abnova, H00002629-M01). **b)** Silver stain of SDS-PAGE-separated proteins from pooled peak fractions from desalting gradient, water wash, and cholate gradient. A protein standard (BioRad, 161-0374) is shown for reference (M).

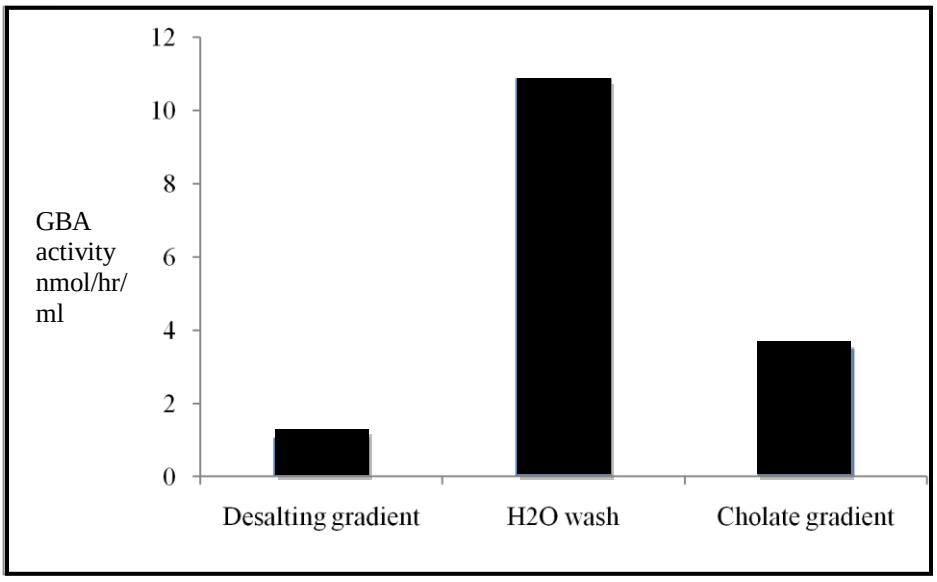

Figure 3.12 Activity of hydrophobic interaction chromatography-purified GBA-PTD from *P. pastoris* induction medium. Activity values in nmol glucose/hr/ml of column elution from peak fractions in desalting gradient, water wash and cholate gradient generated using a natural GBA substrate.

Table 3.1 Purification yield of hydrophobic interaction chromatography (HIC)-purified GBA-PTD4 based on **a)** total GBA activity and **b)** total GBA present as determined by immunoblot band intensity comparison. Band intensity was determined in part from immunoblot shown in Figure 3.11a.

a)

Sample	**Total GBA activity (nmol/hr)**	**Yield (%)**
Crude GBA-PTD4	3016.44	100.00
Post-HIC GBA-PTD4	300.92	9.98

b)

Sample	**Total GBA (µg)**	**Yield (%)**
Crude GBA-PTD4	2222.99	100.00
Post-HIC GBA-PTD4	842.22	37.89

densitometric analysis of immunoblot bands to calculate percent yield. Total GBA amount (µg) was determined from comparison of immunoblot band intensity of GBA-specific bands in post-HIC samples and a pre-column sample. Based on this analysis, it was determined that ~38% of GBA was recovered after purification (Table 3.1b).

HIC fractions from the water wash that contained the majority of active GBA, but that were only partially purified, were pooled, concentrated and subjected to further purification as described in the next section.

3.5.2 Gel filtration chromatography

Gel filtration chromatography (GFC) was used to further purify GBA-PTD4 in HIC water-wash fractions. All GFC column elutions following the void volume (6 ml) were collected and analyzed for activity by 4MUGP assay and protein amount by absorbance at 280 nm. Fractions containing activity were analyzed by SDS-PAGE silver stain and immunoblotting. Two significant peaks in fluorescence corresponding with protein peaks at approximately 9 ml and 11 ml were observed following analysis by 4MUGP assay (Figure 3.13). Visualization of these two peaks by immunoblotting revealed that the majority of GBA was present in fractions from fluorescence peak 1 (Figure 3.14a lane 1) and a small proportion of GBA was present in fractions eluted between peaks 1 and 2 (Figure 3.14a lane 2). No GBA was detected in fractions from peak 2 (Figure 3.14a lanes 4-5). Silver stain analysis revealed that the GBA in peak 1 was eluted with multiple other proteins (Figure 3.14b lanes 1-2) and that pure GBA was exclusively present in the fractions eluted between peaks 1 and 2 (Figure 3.14b lanes 3-4). No protein bands were visible in fractions from the second fluorescence peak (Figure 3.14b lanes 5-6). These data indicate that pure GBA is eluted in the protein peak

a)

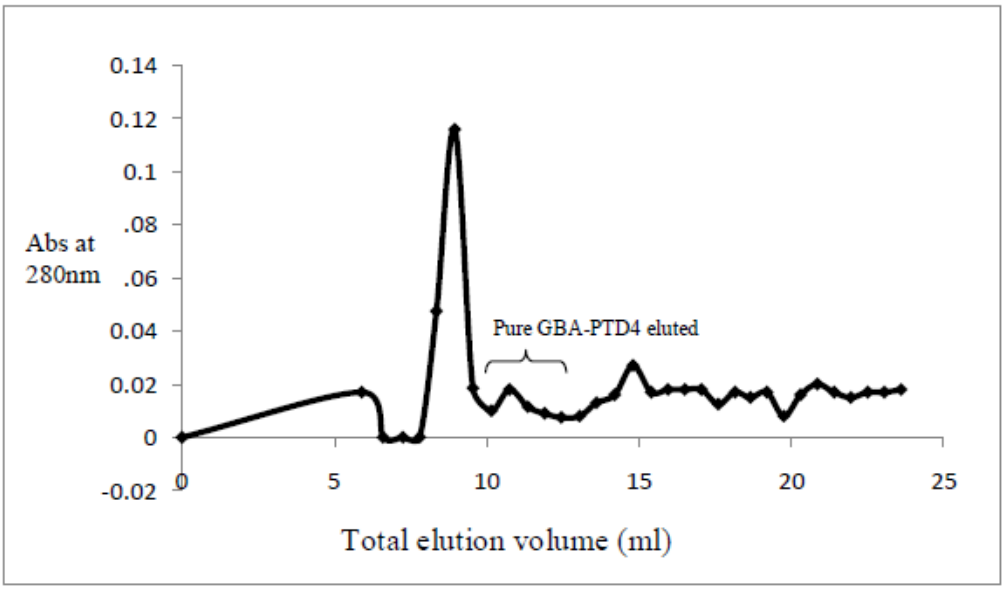

b)

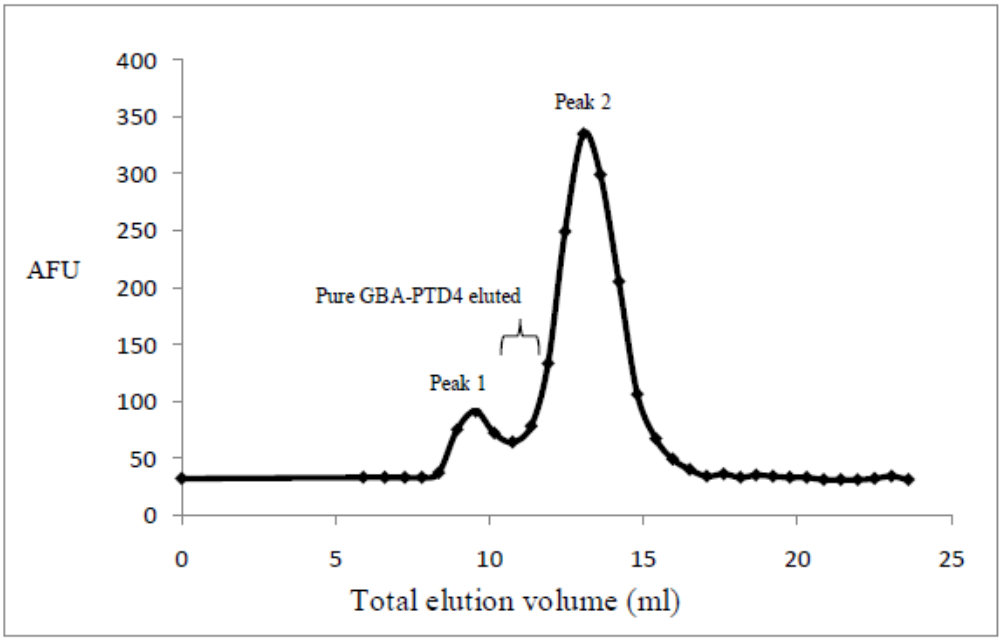

Figure 3.13 Elution profile from gel filtration chromatography of GBA-PTD4 from HIC water-wash fractions. **a)** Absorbance at 280 nm and **b)** fluorescence due to β-glucosidase activity generated from 4MUGP assay of fractions collected over total elution volume.

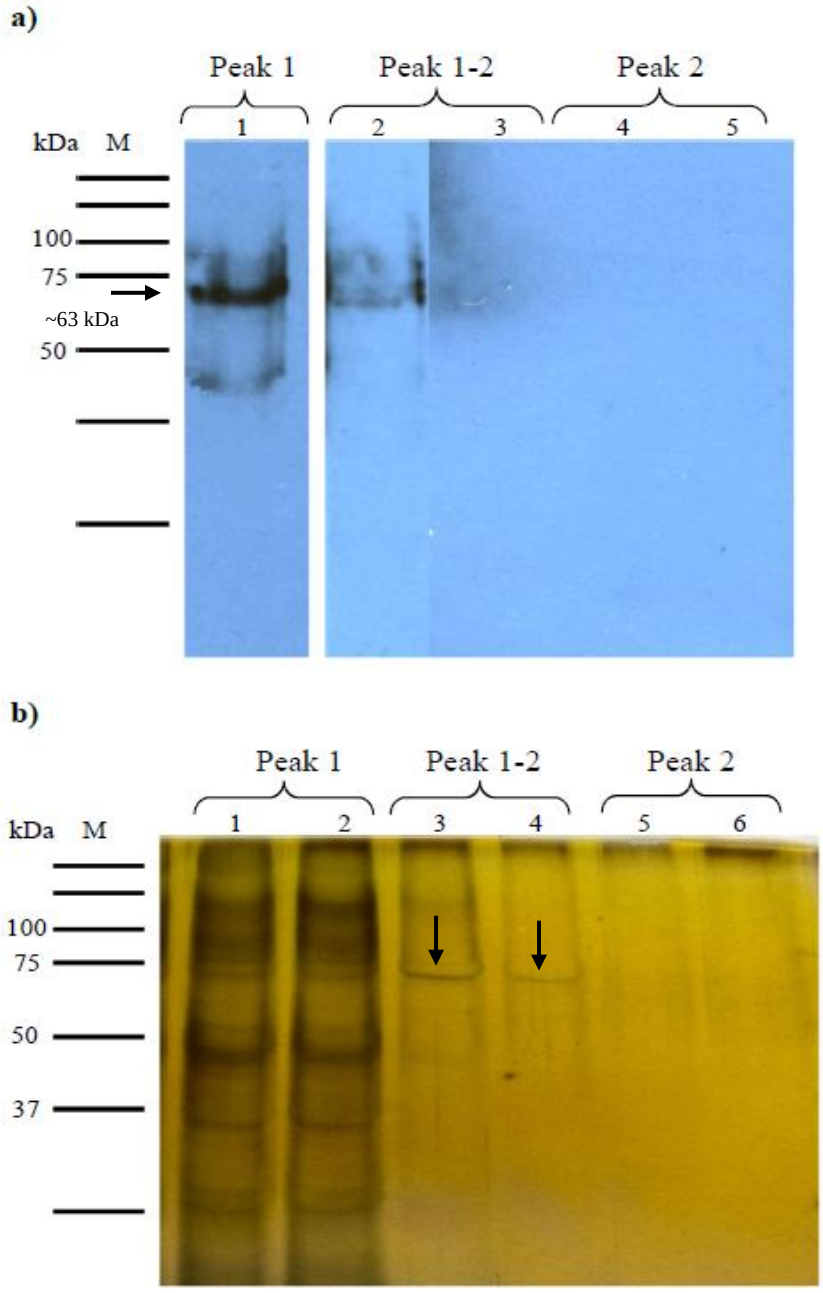

Figure 3.14 Purification of GBA-PTD4 from HIC water-wash fractions by gel filtration chromatography. **a)** Immunoblot of concentrated fractions from fluorescence peaks 1-2. GBA bands (~63 kDa, indicated by arrow) are detected in fractions from peak 1 (lane 1, 45 sec exposure), and fractions from between peaks 1 and 2 (lanes 2-3, overnight exposure), but not in samples from peak 2 (lanes 4-5, overnight exposure). Immuno-detection was performed using an anti-GBA mAb (Abnova, H00002629-M01). **b)** Silver stain of SDS-PAGE separated proteins from concentrated fractions from fluorescence peaks 1-2. Fractions from between peaks 1 and 2 contain a single protein band of approximately 63 kDa (indicated by arrows). A protein standard (BioRad, 161-0374) is shown for reference (M).

corresponding to ~11 ml elution volume.

Activity of pure GBA was not detectable by natural substrate assay due to low sensitivity of the assay and low amounts of active GBA present in post-purification samples. Calculations of purification yield were performed based on total amount of GBA in purified fractions compared to pre-column samples as determined by immunoblot band intensity. A recovery of 2.2% was determined based on this analysis (Table 3.2).

Table 3.2 Purification yield of gel filtration chromatography (GFC)-purified GBA-PTD4 from hydrophobic interaction chromatography (HIC) partially pure fractions. Calculations are based on total GBA present as determined by comparison of immunoblot band intensity. Band intensity was determined in part from immunoblot shown in Figure 3.14a.

Sample	**Total GBA (µg)**	**Yield (%)**
Post-HIC GBA-PTD4	233.00	100.00
GFC-pure GBA-PTD4	5.10	2.19

Chapter 4 – Discussion

This thesis aims to address the work performed on heterologous expression and purification of GBA-PTD4 from *P. pastoris*. This research was conducted to assess the use of *P. pastoris* as an economical alternative to produce recombinant GBA for therapeutic use. In addition, the fusion of a PTD to GBA was performed so that future experiments could assess the use of this domain in transporting GBA across biological membranes, and ultimately for its use in treatment of neurological Gaucher disease. The following sections will discuss results and observations made during expression vector construction, expression studies, and purification runs. Supplementary experiments that could enhance this research, ideas on optimization of protocols, and future projects will also be discussed.

4.1 Expression vector construction

Our three initial GBA expression constructs contained the sequence for a CBD from the exoglucanase Cex protein of *Cellulomonas fimi*. This domain, with its high affinity for cellulose, has been touted for its ability to facilitate purification of enzymes in a single step without disruption of catalytic activity (Richins et al., 2000). CBD was included to investigate if it could represent an alternative purification method for GBA. Previous work in our lab employed a His_6 affinity tag for purification of GBA. This method had little success as the pH required for optimal binding of His_6-tagged proteins to a nickel column was disruptive to GBA activity (Ding, MSc thesis, 2007). Therefore, CBD was suggested as a substitute due to its reported successes in purifications carried out at a broad range of pH values (Terpe, 2003). However, upon discovery of mutations

in CBD-containing constructs, the error-free *GBA*-PTD4 construct was made, which excluded CBD. Other work in our lab with CBD encountered problems with elution of CBD-bound proteins from cellulose columns and cleavage of CBD tags at the incorporated FXa protease recognition site.

GBA cassettes with either N- or C-terminally fused PTD4 were initially constructed, since it was not known if addition of sequence to either terminus would affect conformation. However, at the time of error-free expression cassette construction, the C-terminal PTD4 fusion was chosen. Work published in a similar study where a TAT-peptide was fused to the C-terminus of GBA yielded expression of active enzyme in a mammalian cell system (Lee et al., 2005), thus providing support for our choice to proceed with the C-terminal fusion.

4.2 Verification of transformation by direct yeast PCR

Direct yeast PCR was used to confirm integration of GBA fusion constructs into the *P. pastoris* genome. Vector-specific primers, as opposed to insert-specific primers, were used in direct yeast PCR reactions, as seen in Figure 3.2b and c, to facilitate DNA sequencing of amplicons. However, the use of these primers resulted in amplification of additional products of similar size which posed some complications in terms of identifying the desired GBA bands. AOXI-specific primers, in addition to annealing and amplifying from the pPIC9K vector, can amplify the 2.2 kb endogenous *AOXI* gene. This was problematic when our 2.0 kb band of interest was indistinguishable from the endogenous band. When this situation arose, REN digest was used to identify the contents of the ambiguous PCR product. If GBA was deemed present, a nested PCR using upstream vector-specific α-secretion signal forward and AOXI reverse primers was

performed, followed by sequencing of the amplicons. The other slight complication, as seen in Figure 3.2b, was amplification of an α-mannosidase gene (1.7 kb band) when using vector-specific α-secretion signal forward and 3'AOXI reverse primers. The appearance of this band was unexpected, and only after gel excision and sequencing did its origin become evident. The humanized *P. pastoris* strain was engineered from the commercially available GS115 strain by addition of a vector containing human genes involved in glycosylation (Vervecken et al, 2004). The inserted vector, pGlycoSwitchM5, contained an α-mannosidase gene situated between an *S. cerevisiae* α-secretion signal and an AOXI transcription termination fragment, and was therefore amplified with primers designed for the pPIC9K vector. As long as amplified bands are thoroughly analyzed by restriction digest and/or DNA sequencing, then direct yeast PCR represents an effective method for identifying genomic integration of expression cassettes.

4.3 Protein expression in *P. pastoris*

Optimization of a number of conditions during *P. pastoris* cell culture is essential to successful protein expression. Adjustments in temperature, pH and methanol level during cell culture have been reported to have significant effects on expression of recombinant proteins from *P. pastoris*. The optimal temperature for *P. pastoris* growth is approximately 29°C (Chang et al., 2006). However, a number of important cellular processes in *P. pastoris* are affected by temperature, including protein folding and carbon metabolism (Dragosits et al., 2009). Some researchers have found higher yields of recombinant proteins with less degradation at lower temperatures. Chen et al. (2000) observed increased expression of human α-galactosidase from *P. pastoris* cultured at

25°C compared to 30°C. Similarly, Hong et al. (2002) reported an increase in specific activity of recombinant laccase expressed at 20°C compared to 30°C. This increase in expression of active enzyme was attributed to increased stability and correct folding of recombinant proteins and lower levels of *P. pastoris* proteases in the culture media at lower temperatures (Hong et al., 2002). Expression of recombinant GBA in our study was carried out at 27-28°C. Induction of GBA at lower temperatures may be advantageous in the future to assess the affects of temperature on GBA stability and degradation by proteases.

The pH range for acceptable *P. pastoris* growth is relatively broad (3.0-7.0) (Macauley-Patrick et al., 2005); this allows for pH adjustments to optimize expression of various proteins. Clare et al. (1991) found that a pH of 6.0 in the presence of protease inhibitors was needed for optimal expression of mouse epidermal growth factor from *P. pastoris*. Additionally, a fungal lipase B was optimally expressed at pH values below 5.0; it was suspected that proteolytic degradation was inhibited at lower pH levels (Jahic et al., 2003). Obviously, the chosen pH must be acceptable for stability and activity of the foreign protein being expressed. We therefore conducted *P. pastoris* culturing at pH 5.5 for expression of GBA. This acidic pH is consistent with the pH found in the intra-lysosomal environment and is optimal for GBA stability and activity (Takagi et al., 1999).

Addition of methanol during *P. pastoris* cell culture is essential for transcriptional induction of transgenes under control of the AOXI promoter. The effects of varying amounts of methanol on recombinant protein expression in *P. pastoris* have been investigated. Chen et al. (2000) found that *P. pastoris* growth rates were higher in 1.0%

compared to 3.0% methanol, which is consistent with observations that levels above 1.0% methanol can be toxic to *P. pastoris* cell growth (Minning et al., 2001). Additionally, Hong et al. (2002) found that *P. pastoris* had higher growth rates in 1.0% compared to 0.5% methanol, and observed that increased expression occurred at the lower methanol concentration. Decreased expression at 1.0% methanol was concluded to be due to lower stability and protein folding problems at higher growth rates (Hong et al., 2002). Our experiments involved methanol induction at 0.5% and 1.0% in Mut^+ *P. pastoris* cultures and 1.0% in Mut^S cultures. No formal comparison of growth rate and levels of GBA expression from Mut^+ cultures at these different methanol concentrations were conducted. With respect to Mut^S cultures, we suspect that expression is influenced less by differences in methanol levels due to the inhibited growth of these cells on methanol.

4.3.1 Detecting expression of GBA by activity assay and SDS-PAGE

Two activity assays were applied in this study, the artificial fluorescent substrate 4MUGP assay and the natural GBA lipid substrate assay. The 4MUGP assay is used widely in Gaucher disease research (Ockerman, 1968; Beutler et al., 1971; Sinclair et al., 2006) and was the first assay we employed to detect expression of GBA. This method proved futile for detection of GBA in *P. pastoris* media due to the presence of high background fluorescence caused by endogenous yeast β-glucosidases. The 4MUGP assay represents a sensitive assay for β-glucosidase activity, and therefore was not successful in distinguishing GBA activity in the presence of other enzymes capable of β-glycosidic bond hydrolysis. As shown in Figure 3.4a, fluorescence in medium containing mutant GBA was no higher than in vector-only control medium. Similarly, assays of

media containing error-free GBA yielded no apparent fluorescence above background levels.

The non-specificity of the 4MUGP assay led us to use a natural GBA lipid substrate assay. This assay, although specific for lysosomal GBA, was found to have lower sensitivity than the 4MUGP florescence assay. Low glucose levels produced by cleavage of the substrate would produce unreliable absorbance values after incubation with hexokinase reagents. As a result, samples had to be concentrated before activity was detectable. Concentration was performed by either 40% (w/v) ammonium sulphate precipitation or ultra-filtration using 50,000 MWCO centrifugal devices. The latter method proved to be a more consistent method in terms of producing reproducible results between trials. Additionally, samples were diafiltrated into colourless citrate buffer (pH 5.5) to prevent non-specific absorbance at 340 nm due to the yellow colour of culture medium. It should be noted, however, that slight inconsistencies in colour and concentration were likely present that could have an effect on absorbance readings and subsequent activity results. Other considerations of this assay include its 4-6 hour incubation, and the time and materials required for concentration and diafiltration of samples. This assay, although successful at detecting active GBA expressed from *P. pastoris*, does not represent an ideal method for testing a large number of samples. This was a limiting step in screening multiple colonies with Mut^{+} and Mut^{S} phenotypes when looking for high-expressing clones.

The other method used to investigate GBA expression in our study was SDS-PAGE. Silver stain analysis was an ineffective tool for evaluation of GBA presence. No GBA-sized bands were visible in mutant or error-free GBA samples that were not present

in negative vector-only control samples (Figure 3.4b). This was likely due to a combination of low levels of expressed GBA and the presence of endogenous *P. pastoris* proteins of similar size to GBA. Immunoblot analysis was successful, however, at confirming GBA expression. This method, although revealing nothing about activity, represented the most effective technique for comparing expression levels between several samples since crude medium could be directly contrasted in a single blot and multiple blots could be performed simultaneously under identical conditions. However, if future optimization experiments seek to compare numerous *GBA*-containing *P. pastoris* clones cultured under varying conditions, an alternate expression detection method would prove essential. Protein dot-blotting could be used to efficiently detect the presence of GBA in a large number of samples concurrently. Protein dot-blots are useful for high-throughput evaluation of non-enzymatic proteins or enzymes when no effective or efficient activity assay is available (Galperin et al., 2004; Zeder-Lutz et al., 2006). For example, Zeder-Lutz et al. (2006) developed a sensitive, high-throughput dot-blot immunodetection assay to assess expression of one hundred G-protein-coupled receptors in *P. pastoris.*

4.3.2 Expression of mutant GBA

Attempts to express the GBA fusions CBD-*GBA*, CBD-PTD4-*GBA*, and CBD-*GBA*-PTD4 were performed prior to knowledge that these constructs contained mutations in the *GBA* cDNA. Low levels of enzyme with undetectable activity and significant apparent degradation were observed (Figures 3.4 and 3.6). Two missense mutations identified in all three of these constructs, in exons 4 and 7, were suspected to be responsible for the low yield of active enzyme, presumably by affecting conformation and stability of the resulting polypeptide. Upon correction of the altered nucleotides, it

was observed that expression levels increased and enzyme activity was detectable (Figures 3.7 and 3.9). To confirm that increased expression was due to correction of the mutations and not due to the absence of CBD in the newly generated *GBA*-PTD4 construct, we compared the amount of GBA expressed from mutant and error-free *GBA*-PTD4 constructs.

It is impossible to know the exact effect that the identified mutations had on GBA without performing functional characterization. However, based on our observations, the location of each mutation in the *GBA* gene, the type of amino acid change, and published reports of similar mutations, we can presume that each mutation had some effect on activity and stability of GBA. The mutation that we identified in *GBA* exon 4 consists of a G-to-A change resulting in an alteration from non-polar, small R-group-containing alanine to polar threonine at amino acid position 84 (A84T). This mutation occurs next to amino acid position 85 in which a M85T mutation has been reported (Hruska et al., 2008). Unfortunately details on this finding were not published and no information on the severity of the mutation is available. However, we entertain the possibility that our A84T mutation may be mild based on reports of an identical alanine to threonine amino acid change at position 90 (Koprivica et al., 2000). This A90T mutation was reported in a type I GD patient in combination with a well-characterized severe mutation indicating that A90T is likely mild in consequence (Koprivica et al., 2000).

The mutation found in *GBA* exon 7 was a T-to-G change resulting in a switch from non-polar leucine to significantly larger, positively-charged arginine at position 264 (L264R). This mutation is located next to amino acid 265, where a G265D mutation has been recorded in a survey paper of Argentinean GD patients. The G265D mutation was

reported in siblings in conjunction with N370S (Cormand et al., 1998). These type I GD patients presented with splenomegaly at 19 and 12 years of age (Cormand et al., 1998). This case report gives little insight into the severity of G265D and therefore there is little to be deduced about L264R. However, another study identifies a type II GD-mutation cluster region nearby in exon 7 between amino acid positions 250 and 259, indicating that mutations in exon 7 can have severe effects on GBA functionality (Tang et al., 2005).

An exon 8 T-to-C mutation was found exclusively in our CBD-PTD4-*GBA* construct. This nucleotide change resulted in an alteration from non-polar, sulphur-containing methionine to polar threonine at amino acid position 361 (M361T). A tyrosine-to-cysteine mutation nearby at amino acid position 363 (Y363C) was reported in a type II GD patient who died at 15 months of age (Tang et al., 2005). Functional characterization of the Y363C mutation revealed that the resulting GBA polypeptide exhibited a major loss of catalytic activity (Tang et al., 2005). These data suggest that M361T likely results in significant GBA disruption. It is also interesting to note that GBA containing all three mutations appeared more severely degraded than GBA containing the A84T and L264R mutations only (Figure 3.6).

We suspect that the combination of A84T, L264R, and M361T resulted in decreased enzyme activity due to conformational changes and reduction in polypeptide stability leading to increased degradation and overall low levels of secreted and intracellular enzyme.

4.3.3 Expression of error-free GBA

Expression of error-free GBA-PTD4 yielded three protein species of approximately 63, 45, and 35 kDa. The 63 kDa product is the expected size of full-length

GBA with correct glycosylation (Berg-Fussman et al., 1993). The humanized *P. pastoris* strain was used in our study for production of human GBA due to its reported ability to produce heterologous proteins with mammalian-like glycosylation (Vervecken et al., 2004). Analysis of glycosylation on GBA-PTD4 should be performed in future to confirm correct type and approximate size of the added glucosyl residues. A reduction in size to approximately 55 kDa following digestion of oligosaccharide residues would indicate that the desired amount of glycosylation was performed (Berg-Fussman et al., 1993). Correct glycosylation is essential to enzyme function and preventing immunogenicity if a glycoprotein is destined for therapeutic use. Shaaltiel et al. (2007) analyzed glycan structure of recombinant GBA expressed in plant cells by sequential digestion with various exoglycosidases before proceeding to testing the effectiveness the enzyme in a GD mouse model.

In addition to expression of the full-sized GBA polypeptide, two bands of approximately 45 and 35 kDa were consistently present in anti-GBA immunoblots (Figures 3.7 and 3.8). The smaller protein bands were confirmed to be derived from GBA by absence of anti-GBA cross-reactive bands in negative control medium (vector only), and absence of bands when GBA samples were probed with an anti-His monoclonal antibody (data not shown). These smaller GBA bands are suspected to originate from post-translational degradation rather than alternative splicing of GBA. Immunoblot intensity of the smaller GBA bands was less in samples of freshly harvested medium compared to medium that had been processed and exposed to unfavourable conditions such as during concentration and purification. The observation that the amount of degraded enzyme seemed to increase in post-harvest medium suggests that the

degradation is likely due to proteases present in the medium and that the degradation is occurring after GBA is secreted. A number of yeast extracellular proteases have been characterized (Ogrydziak, 1993); however, reports that few proteins are secreted from *P. pastoris* (Cereghino and Cregg, 2000) have led to the belief that the most common agents of proteolysis in *P. pastoris* are vacuolar proteases (Macauley-Patrick et al., 2005; Sinha et al., 2005). GBA degradation is presumably occurring upon release of vacuolar proteases when cells lyse in culture. In a study investigating the causes of proteolytic degradation in *P. pastoris*, Sinha et al. (2005) found that during methanol induction, levels of vacuolar proteases in culture medium increased substantially after 48 hours. The presence of proteases after this time point was concluded to be due to cell lysis as cultures entered stationary phase (Sinha et al., 2005). This supports our observations that samples harvested at earlier time points appear to have less degraded protein than samples from later time points (Figure 3.7 and 3.8).

A number of strategies exist to inhibit proteases, such as addition of casamino acids as an alternate substrate (Clare et al., 1991), addition of protease inhibitors (Jahic et al., 2003), and use of protease-deficient *P. pastoris* strains (Brankamp et al., 1995). Clare et al. (1991) reported that addition of 1% (w/v) casamino acids and buffering to pH 6.0 resulted in increased levels of secreted mouse epidermal growth factor due to reduced proteolytic degradation under these conditions. Addition of protease inhibitors to *P. pastoris* induction media or cell lysates has also been successful in reducing proteolytic degradation of certain recombinant proteins. A study on the inhibition of *P. pastoris* proteases found that a combination of a serine protease inhibitor and a metalloprotease inhibitor resulted in 94% reduction in protease activity (Sinha et al., 2005). This report

also noted that additional classes of proteases, such as aspartic proteases, that are active at various pH, are present intracellularly in *P. pastoris* as well as in the culture medium (Sinha et al., 2005). It could therefore be relevant to test various combinations of protease inhibitors to investigate their effect on reducing degradation of GBA expressed by *P. pastoris*. Additionally, several protease-deficient *P. pastoris* strains have been developed. These strains contain defective proteinase A, one of the principle vacuolar proteases required for proteolytic degradation in *P. pastoris* (Reviewed by Van Den Hazel et al., 1996). Various researchers have reported decreased proteolytic breakdown of their recombinant proteins when using a protease-deficient strain (Brankamp et al., 1995; Sreekrishna et al., 1997). Expression of GBA in such a host could be performed to conclude whether proteolytic action due to vacuolar proteases is responsible for the smaller GBA bands that we observed.

In terms of full-length GBA, our results show optimal expression at approximately 48 hours of induction (Figure 3.7 and 3.8). No GBA was detected in samples harvested after ~77 hours (Figure 3.8). We presume that levels of full-length GBA decreased after 48 hours due to increased levels of proteases in culture medium, and increased pH of medium at later time points. Clare et al. (1991) reported a shift in pH from 6.0 to 8.0 during induction, and similarly we observed an increase in culture medium pH over time. This shift towards basic pH has adverse effects on GBA stability (Pentchev et al., 1973). Therefore, it is important to note that the optimal time point for expression is pH dependent, in part, and adjustments in pH during induction would likely yield variable optimal expression time points.

Additionally, optimal expression of active GBA was observed from Mut^S clones compared to Mut^+ clones (Figure 3.8 and 3.9). Interestingly, Mut^+ cells are most commonly used for heterologous protein expression due to their rapid growth rate and ability to drive expression of foreign proteins when grown with methanol (Cereghino and Cregg, 2000). Conversely, cells with the methanol utilization slow phenotype have impaired growth on methanol due to a disrupted *AOXI* gene; this can be advantageous, however, for production of proteins that are toxic to host cells, or that require complex post-translational modifications (Sinclair and Choy, 2002; Daly and Hearn, 2005; Emberson et al., 2005). The necessity for post-translational glycosylation of GBA may explain why expression was favourable in Mut^S cells. To further investigate expression in Mut^+ and Mut^S hosts, transgene copy number should be considered. The pPIC9K vector used in our study allows multiple expression-vector integration events into the host genome by homologous recombination. Numerous reports indicate that increased gene dosage results in increased levels of recombinant proteins (Clare et al., 1991; Chen et al., 2000). For example Clare et al. (1991) selected a 19x integrant that was capable of producing 450 µg/ml of heterologous protein in fermentation cultures. However, others report that increased copy number can have adverse effects on expression due to a limitation of resources needed for transcription, translation and post-translation modifications of multiple genes under the control of a strong promoter (Macauley-Patrick et al., 2005). One study observed increased expression of recombinant trypsinogen in a 2x integrant, but decreased protein levels were observed in clones with more than two gene copies (Hohenblum et al., 2004). In our study, we selected a Mut^+ transformant

with more than 2 integrated copies of *GBA*. Future experiments should compare multiple and single *GBA* integrant clones in both Mut^+ and Mut^S strains.

The observed expression of GBA-PTD4 from *P. pastoris* is encouraging with respect to the use of this system for production of GBA for therapeutic use. However, we conclude that the levels of expressed GBA-PTD4 must be increased so further analysis and characterization of this fusion enzyme can be conducted. We propose that optimization of culture conditions is warranted and application of protease inhibition is advisable for future experiments and before large scale production using fermentor technology is conducted.

4.4 Purification of GBA-PTD4

4.4.1 Hydrophobic interaction chromatography

HIC was used to purify GBA-PTD4 from *P. pastoris* induction medium. This method elutes proteins based on their hydrophobicity and is therefore effective at separating strongly hydrophobic proteins, such as GBA, from other proteins present in culture medium. HIC has been used to purify GBA expressed in insect (Sinclair et al., 2006) and plant cell systems (Shaaltiel et al., 2007), sometimes in combination with a second purification step such as ion-exchange chromatography. Previous work in our lab reported purification of His_6-tagged GBA from humanized *P. pastoris,* with pure GBA eluted early in the cholate gradient (Ding, 2007, MSc thesis). Our results in the current study show the majority of GBA eluting from the column in the water wash along with other moderately hydrophobic proteins and continued GBA elution into the cholate gradient, where fractions contain much less, if any, contaminating proteins (Figure 3.11). No visible immunoblot cross-reactive GBA bands were seen in samples from the desalting gradient (Figure 3.11), although it should be noted that film exposure for

extended periods did reveal presence of GBA, albeit in low amounts. We therefore conclude that GBA was not eluted in a single peak, but rather in several protein peaks ranging from the end of the desalting gradient (typically in the transition from 100% buffer B to 100% water) to the beginning of the cholate gradient (~0-0.75% cholate). We suspect that the decreased hydrophobic behaviour observed is due to the addition of PTD4. We propose that the additional basic domain results in weaker hydrophobic interactions of the fusion enzyme to the column matrix, resulting in earlier and more dispersed elution. However, in attempts to improve separation of GBA, future HIC runs will involve commencement of the water wash phase only after the protein peaks from the desalting gradient have returned to baseline.

It should be noted that some degraded GBA appears to be co-purified along with full-length GBA, indicating that these degraded fragments retain a similar hydrophobic profile to intact GBA. Although the blot present in Figure 3.11a indicates only very faint degraded GBA bands, longer exposures showed clear presence of these bands (not shown).

Detecting activity in HIC-purified samples was performed by 4MUGP and natural substrate assay. The former assay fails to distinguish GBA activity from total β-glucosidase activity, but suggests which fractions contain GBA, either in the pure form or in combination with other β-glycosidic enzymes and contaminating proteins. Figure 3.10b shows two significant fluorescence peaks indicative of β-glucosidase activity, one in the desalting gradient and one in the water wash. Immunoblot analysis of the desalting gradient fluorescence peak revealed that these fractions did not contain GBA protein (Figure 3.11a). We therefore conclude that the β-glucosidase activity in these fractions is

due to non-specific endogenous β-glucosidase enzymes that eluted from the column at this point and were effectively separated from GBA. The fluorescence peak in the water wash did contain GBA, in addition to a number of contaminating proteins (Figure 3.11). Fractions containing β-glucosidase activity, as determined by the 4MUGP assay, were tested for GBA activity using the natural substrate assay. The activity results confirmed what was seen in immunoblots by revealing GBA activity in the water wash and cholate gradient as well as low amounts in tail desalting gradient fractions (Figure 3.12). It was suspected that activity levels in purified samples compared to crude samples would be lower due to increased enzyme instability in the purified form. This was supported by comparison of purification yield calculated using total GBA activity to total GBA protein. The yield calculated from activity data reported ~10% enzyme recovery, whereas the yield based on total GBA protein, irrespective of activity, was ~38%. This indicated that GBA is subject to loss of activity in the purified form.

4.4.2 Gel filtration chromatography

Gel filtration chromatography was used to further separate partially purified GBA samples based on size. GFC is often employed as a final purification step in attempts to achieve homogenous protein. Previous experiments in our lab using HIC followed by GFC to purify GBA from insect cell culture media reported pure GBA eluted from the GFC column at around 14-15 ml (Deacon, 2003, BSc Hons thesis). Results from the current work report pure GBA eluted at ~11 ml elution volume. Significant loss of GBA was observed during GFC. A large amount of non-purified GBA appeared to be excluded from the column while only part of the applied sample seemed to enter the column matrix and be separated effectively.

As with HIC, GFC fractions were analyzed for activity initially by 4MUGP assay and subsequently by natural substrate assay. The latter method was not sensitive enough to detect GBA activity in GFC fractions, likely due to insufficient amounts of active GBA in these samples. 4MUGP analysis revealed two major fluorescence peaks that were subsequently investigated by immunoblot and silver stain (Figure 3.14). SDS-PAGE analysis illustrated that the first fluorescence peak contained GBA with many contaminating proteins, while the second fluorescence peak contained proteins that were not visible when analyzed by SDS-PAGE, but likely included non-specific yeast β-glucosidases and potentially small amounts of GBA. Pure GBA was eluted between peaks 1 and 2; the low activity seen in these samples supports the idea that pure enzyme is unstable and undergoes a time-dependent irreversible loss of catalytic activity. Since no activity data was available for pure fractions, percent yield was calculated based on total GBA present in pure fractions compared to pre-column samples as determined by densitometric immunoblot band comparison. It was determined that GFC resulted in approximately 2.2% recovery of GBA. This low yield is explained in part by the observed loss of GBA by elution in the earlier, non-pure fractions. Protein purification fold was not included in this study since the calculated values were not representative of actual purification since they were based on activity, which was significantly decreased in purified samples.

GFC appears to be an effective method for separation of GBA that actually enter the column matrix, therefore future attempts should focus on preventing loss of sample through the use of new columns and a more uniform sample application method.

4.5 Conclusions and future directions

Recombinant GBA-PTD4 was successfully expressed in *P. pastoris* and purified to apparent homogeneity by use of two purification steps. Analysis of expression revealed that GBA-PTD4 was expressed in higher amounts in cells with the Mut^S phenotype. Only one clone of each methanol utilization phenotype was used; therefore, future experiments should involve screening multiple clones with variable gene copy numbers for identification of high expressing transformants. Time point studies showed that 48 hours post methanol induction was the optimal time to harvest culture medium as these samples contained the most full-length GBA with the highest activity. However, the optimal expression time point should be re-assessed if culture conditions are changed in future experiments. Two smaller-than-expected GBA species were consistently present. The cause of these products is suspected to be proteolytic degradation. Further experiments should focus on inhibition of *P. pastoris* proteases in attempts to achieve higher levels of full-length GBA-PTD4.

In addition to various optimization experiments, future research should include large-scale expression of GBA-PTD4 using fermentor technology. Bioreactors for culturing *P. pastoris* at extremely high cell densities should be applied for cost-effective production of GBA-PTD4 for therapeutic use.

Optimizing purification of GBA-PTD4 from *P. pastoris* induction media will also be an important focus of future experiments. In addition to HIC and GFC, other potentially more effective purification methods, such as immunopurification using anti-GBA or anti-PTD mAbs, could be explored.

The reality of using GBA-PTD4 as a treatment for neurological Gaucher disease must also be addressed in the future. Safety and effectiveness are two principle

considerations for the use of this fusion enzyme as a human therapeutic. Human recombinant GBA from mammalian cells is currently used by patients (Brady, 2003), and human GBA expressed in carrot cells has recently entered clinical trials after toxicity was studied in mice (Shaaltiel et al., 2007). Additionally, application of PTD fusion drugs in rodents have had reported success with few adverse immunological effects noted thus far (Elliger et al., 2002; Kilic et al., 2003). In terms of efficacy, the ability of PTD4 to transport GBA across biological membranes must be assessed. Initial *in vitro* cellular uptake studies should be conducted; human Gaucher patient skin fibroblasts would represent an effective model to investigate the transduction capability of GBA-PTD4 into cultured cells. These cells lack surface mannose-6-phosphate receptors, thus restricting uptake to PTD4 facilitated methods (Zhang et al., 2008). Subsequent, application of GBA-PTD4 in a GD mouse would be necessary to test delivery into the brain. It is important to note that drug delivery facilitated by PTDs is not brain specific. This may represent a disadvantage for certain drugs where a specific target location is required. However, entry of GBA-PTD4 into non-neuronal cells in addition to cells of the CNS would be advantageous for GD patients. Additionally, it has been reported that replacement of only 15-20% of GBA activity is needed for clinical efficacy (Beck, 2007). If GBA-PTD4 is successful in penetrating the BBB, the effectiveness of the enzyme to degrade accumulated substrate and reverse disease symptoms or slow disease progression must be evaluated.

Bibliography

Aerts JM, Hollak CE, Boot RG, Groener JE, Maas M (2006) Substrate reduction therapy of glycosphingolipid storage disorders. J Inherit Metab Dis 29:449-456.

Alterini R, Rigacci L, Stefanacci S (1996) Pseudo-Gaucher cells in the bone marrow of a patient with centrocytic nodular non-Hodgkin's lymphoma. Haematologica 81:282-283.

Balicki D, Beutler E (1995) Gaucher disease. Medicine (Baltimore) 74:305-323.

Barton NW, Furbish FS, Murray GJ, Garfield M, Brady RO (1990) Therapeutic response to intravenous infusions of glucocerebrosidase in a patient with Gaucher disease. Proc Natl Acad Sci U S A 87:1913-1916.

Beck M (2007) New therapeutic options for lysosomal storage disorders: enzyme replacement, small molecules and gene therapy. Hum Genet 121:1-22.

Berg-Fussman A, Grace ME, Ioannou Y, Grabowski GA (1993) Human acid beta-glucosidase. N-glycosylation site occupancy and the effect of glycosylation on enzymatic activity. J Biol Chem 268:14861-14866.

Beutler E (2006) Lysosomal storage diseases: natural history and ethical and economic aspects. Mol Genet Metab 88:208-215.

Beutler E, Kuhl W (1970) The diagnosis of the adult type of Gaucher's disease and its carrier state by demonstration of deficiency of beta-glucosidase activity in peripheral blood leukocytes. J Lab Clin Med 76:747-755.

Beutler E, Grabowski GA (2001) Gaucher Disease. In: The Metabolic and Molecular Bases of Inherited Disease, 8th Edition (Scriver CR, Beaudet AL, Sly WS, Valle D, eds), pp 3635-3668. New York: McGraw Hill.

Beutler E, Kuhl W, Trinidad F, Teplitz R, Nadler H (1971) Beta-glucosidase activity in fibroblasts from homozygotes and heterozygotes for Gaucher's disease. Am J Hum Genet 23:62-66.

Beutler E, Gelbart T, Kuhl W, Zimran A, West C (1992) Mutations in Jewish patients with Gaucher disease. Blood 79:1662-1666.

Boot RG, Verhoek M, de Fost M, Hollak CE, Maas M, Bleijlevens B, van Breemen MJ, van Meurs M, Boven LA, Laman JD, Moran MT, Cox TM, Aerts JM (2004) Marked elevation of the chemokine CCL18/PARC in Gaucher disease: a novel surrogate marker for assessing therapeutic intervention. Blood 103:33-39.

Brady RO (1966) The sphingolipidoses. N Engl J Med 275:312-318.

Brady RO (2003) Enzyme replacement therapy: conception, chaos and culmination. Philos Trans R Soc Lond B Biol Sci 358:915-919.

Brady RO, Kanfer JN, Shapiro D (1965) Metabolism of Glucocerebrosides. Ii. Evidence of an Enzymatic Deficiency in Gaucher's Disease. Biochem Biophys Res Commun 18:221-225.

Brankamp RG, Sreekrishna K, Smith PL, Blankenship DT, Cardin AD (1995) Expression of a synthetic gene encoding the anticoagulant-antimetastatic protein ghilanten by the methylotropic yeast Pichia pastoris. Protein Expr Purif 6:813-820.

Cereghino JL, Cregg JM (2000) Heterologous protein expression in the methylotrophic yeast Pichia pastoris. FEMS Microbiol Rev 24:45-66.

Chang SW, Shieh CJ, Lee GC, Akoh CC, Shaw JF (2006) Optimized growth kinetics of Pichia pastoris and recombinant Candida rugosa LIP1 production by RSM. J Mol Microbiol Biotechnol 11:28-40.

Chen Y, Jin M, Egborge T, Coppola G, Andre J, Calhoun DH (2000) Expression and characterization of glycosylated and catalytically active recombinant human alpha-galactosidase A produced in Pichia pastoris. Protein Expr Purif 20:472-484.

Choy FY, Davidson RG (1980) Gaucher disease. III. Substrate specificity of glucocerebrosidase and the use of nonlabeled natural substrates for the investigation of patients. Am J Hum Genet 32:670-680.

Choy FY, Woo M (1991) Purification and the effect of peptide N-glycosidase F on lysosomal membrane-bound glucocerebrosidase from human cultured fibroblasts. Biochem Cell Biol 69:551-556.

Clare JJ, Romanos MA, Rayment FB, Rowedder JE, Smith MA, Payne MM, Sreekrishna K, Henwood CA (1991) Production of mouse epidermal growth factor in yeast: high-level secretion using Pichia pastoris strains containing multiple gene copies. Gene 105:205-212.

Cormand B, Harboe TL, Gort L, Campoy C, Blanco M, Chamoles N, Chabas A, Vilageliu L, Grinberg D (1998) Mutation analysis of Gaucher disease patients from Argentina: high prevalence of the RecNciI mutation. Am J Med Genet 80:343-351.

Cox TM (2001) Gaucher disease: understanding the molecular pathogenesis of sphingolipidoses. J Inherit Metab Dis 24 Suppl 2:106-121; discussion 187-108.

Cox TM, Schofield JP (1997) Gaucher's disease: clinical features and natural history. Baillieres Clin Haematol 10:657-689.

Cox TM, Aerts JM, Andria G, Beck M, Belmatoug N, Bembi B, Chertkoff R, Vom Dahl S, Elstein D, Erikson A, Giralt M, Heitner R, Hollak C, Hrebicek M, Lewis S, Mehta A, Pastores GM, Rolfs A, Miranda MC, Zimran A (2003) The role of the iminosugar N-butyldeoxynojirimycin (miglustat) in the management of type I (non-neuronopathic) Gaucher disease: a position statement. J Inherit Metab Dis 26:513-526.

Daly R, Hearn MT (2005) Expression of heterologous proteins in Pichia pastoris: a useful experimental tool in protein engineering and production. J Mol Recognit 18:119-138.

Davson H (1976) Review lecture. The blood-brain barrier. J Physiol 255:1-28.

Deacon DR (2003) HIC, GPC and GBA: A process for the Purification of Acid beta-Glucosidase. In: University of Victoria.

Dean N (1999) Asparagine-linked glycosylation in the yeast Golgi. Biochim Biophys Acta 1426:309-322.

Ding W (2007) Expression of glucocerebrosidase in humanized *Pichia pastoris* expression system and protein purification

In: University of Victoria.

Dinur T, Osiecki KM, Legler G, Gatt S, Desnick RJ, Grabowski GA (1986) Human acid beta-glucosidase: isolation and amino acid sequence of a peptide containing the catalytic site. Proc Natl Acad Sci U S A 83:1660-1664.

Dragosits M, Stadlmann J, Albiol J, Baumann K, Maurer M, Gasser B, Sauer M, Altmann F, Ferrer P, Mattanovich D (2009) The effect of temperature on the proteome of recombinant Pichia pastoris. J Proteome Res 8:1380-1392.

Duchardt F, Fotin-Mleczek M, Schwarz H, Fischer R, Brock R (2007) A comprehensive model for the cellular uptake of cationic cell-penetrating peptides. Traffic 8:848-866.

Dvir H, Harel M, McCarthy AA, Toker L, Silman I, Futerman AH, Sussman JL (2003) X-ray structure of human acid-beta-glucosidase, the defective enzyme in Gaucher disease. EMBO Rep 4:704-709.

Eblan MJ, Goker-Alpan O, Sidransky E (2005) Perinatal lethal Gaucher disease: a distinct phenotype along the neuronopathic continuum. Fetal Pediatr Pathol 24:205-222.

Elliger SS, Elliger CA, Lang C, Watson GL (2002) Enhanced secretion and uptake of beta-glucuronidase improves adeno-associated viral-mediated gene therapy of mucopolysaccharidosis type VII mice. Mol Ther 5:617-626.

Emberson LM, Trivett AJ, Blower PJ, Nicholls PJ (2005) Expression of an anti-CD33 single-chain antibody by Pichia pastoris. J Immunol Methods 305:135-151.

Enquist IB, Nilsson E, Ooka A, Mansson JE, Olsson K, Ehinger M, Brady RO, Richter J, Karlsson S (2006) Effective cell and gene therapy in a murine model of Gaucher disease. Proc Natl Acad Sci U S A 103:13819-13824.

Enquist IB, Lo Bianco C, Ooka A, Nilsson E, Mansson JE, Ehinger M, Richter J, Brady RO, Kirik D, Karlsson S (2007) Murine models of acute neuronopathic Gaucher disease. Proc Natl Acad Sci U S A 104:17483-17488.

Erickson AH, Ginns EI, Barranger JA (1985) Biosynthesis of the lysosomal enzyme glucocerebrosidase. J Biol Chem 260:14319-14324.

Fawell S, Seery J, Daikh Y, Moore C, Chen LL, Pepinsky B, Barsoum J (1994) Tat-mediated delivery of heterologous proteins into cells. Proc Natl Acad Sci U S A 91:664-668.

Fischer H, Gottschlich R, Seelig A (1998) Blood-brain barrier permeation: molecular parameters governing passive diffusion. J Membr Biol 165:201-211.

Frankel AD, Pabo CO (1988) Cellular uptake of the tat protein from human immunodeficiency virus. Cell 55:1189-1193.

Galperin MM, Traicoff JL, Ramesh A, Freebern WJ, Haggerty CM, Hartmann DP, Emmert-Buck MR, Gardner K, Knezevic V (2004) Multimembrane dot-blotting: a cost-effective tool for proteome analysis. Biotechniques 36:1046-1051.

Gaucher P (1882) De l'epithelioma primitif de la rate, hpertrophie idiopathique de la rate sans leucemie In: Thesis. Paris.

Gellissen G, Melber K, Janowicz ZA, Dahlems UM, Weydemann U, Piontek M, Strasser AW, Hollenberg CP (1992) Heterologous protein production in yeast. Antonie Van Leeuwenhoek 62:79-93.

Gemmill TR, Trimble RB (1999) Overview of N- and O-linked oligosaccharide structures found in various yeast species. Biochim Biophys Acta 1426:227-237.

Glew RH, Basu A, LaMarco KL, Prence EM (1988) Mammalian glucocerebrosidase: implications for Gaucher's disease. Lab Invest 58:5-25.

Green M, Loewenstein PM (1988) Autonomous functional domains of chemically synthesized human immunodeficiency virus tat trans-activator protein. Cell 55:1179-1188.

Hamilton SR, Bobrowicz P, Bobrowicz B, Davidson RC, Li H, Mitchell T, Nett JH, Rausch S, Stadheim TA, Wischnewski H, Wildt S, Gerngross TU (2003) Production of complex human glycoproteins in yeast. Science 301:1244-1246.

Hamilton SR, Davidson RC, Sethuraman N, Nett JH, Jiang Y, Rios S, Bobrowicz P, Stadheim TA, Li H, Choi BK, Hopkins D, Wischnewski H, Roser J, Mitchell T, Strawbridge RR, Hoopes J, Wildt S, Gerngross TU (2006) Humanization of yeast to produce complex terminally sialylated glycoproteins. Science 313:1441-1443.

Higgins DR, Cregg JM (1998) Introduction to Pichia pastoris. Methods Mol Biol 103:1-15.

Ho A, Schwarze SR, Mermelstein SJ, Waksman G, Dowdy SF (2001) Synthetic protein transduction domains: enhanced transduction potential in vitro and in vivo. Cancer Res 61:474-477.

Hohenblum H, Gasser B, Maurer M, Borth N, Mattanovich D (2004) Effects of gene dosage, promoters, and substrates on unfolded protein stress of recombinant Pichia pastoris. Biotechnol Bioeng 85:367-375.

Hollak CE, Evers L, Aerts JM, van Oers MH (1997) Elevated levels of M-CSF, sCD14 and IL8 in type 1 Gaucher disease. Blood Cells Mol Dis 23:201-212.

Hong F, Meinander NQ, Jonsson LJ (2002) Fermentation strategies for improved heterologous expression of laccase in Pichia pastoris. Biotechnol Bioeng 79:438-449.

Horowitz M, Wilder S, Horowitz Z, Reiner O, Gelbart T, Beutler E (1989) The human glucocerebrosidase gene and pseudogene: structure and evolution. Genomics 4:87-96.

Hruska KS, LaMarca ME, Scott CR, Sidransky E (2008) Gaucher disease: mutation and polymorphism spectrum in the glucocerebrosidase gene (GBA). Hum Mutat 29:567-583.

Huynh GH, Deen DF, Szoka FC, Jr. (2006) Barriers to carrier mediated drug and gene delivery to brain tumors. J Control Release 110:236-259.

Jahic M, Gustavsson M, Jansen AK, Martinelle M, Enfors SO (2003) Analysis and control of proteolysis of a fusion protein in Pichia pastoris fed-batch processes. J Biotechnol 102:45-53.

Kampine JP, Brady RO, Kanfer JN, Feld M, Shapiro D (1967) Diagnosis of gaucher's disease and niemann-pick disease with small samples of venous blood. Science 155:86-88.

Kilic U, Kilic E, Dietz GP, Bahr M (2003) Intravenous TAT-GDNF is protective after focal cerebral ischemia in mice. Stroke 34:1304-1310.

Koprivica V, Stone DL, Park JK, Callahan M, Frisch A, Cohen IJ, Tayebi N, Sidransky E (2000) Analysis and classification of 304 mutant alleles in patients with type 1 and type 3 Gaucher disease. Am J Hum Genet 66:1777-1786.

Kornfeld S (1986) Trafficking of lysosomal enzymes in normal and disease states. J Clin Invest 77:1-6.

Lachmann RH, Grant IR, Halsall D, Cox TM (2004) Twin pairs showing discordance of phenotype in adult Gaucher's disease. QJM 97:199-204.

Lee KO, Luu N, Kaneski CR, Schiffmann R, Brady RO, Murray GJ (2005) Improved intracellular delivery of glucocerebrosidase mediated by the HIV-1 TAT protein transduction domain. Biochem Biophys Res Commun 337:701-707.

Macauley-Patrick S, Fazenda ML, McNeil B, Harvey LM (2005) Heterologous protein production using the Pichia pastoris expression system. Yeast 22:249-270.

Meivar-Levy I, Horowitz M, Futerman AH (1994) Analysis of glucocerebrosidase activity using N-(1-[14C]hexanoyl)-D-erythroglucosylsphingosine demonstrates a correlation between levels of residual enzyme activity and the type of Gaucher disease. Biochem J 303 (Pt 2):377-382.

Mignot C, Gelot A, Bessieres B, Daffos F, Voyer M, Menez F, Fallet Bianco C, Odent S, Le Duff D, Loget P, Fargier P, Costil J, Josset P, Roume J, Vanier MT, Maire I, Billette de Villemeur T (2003) Perinatal-lethal Gaucher disease. Am J Med Genet A 120A:338-344.

Minning S, Serrano A, Ferrer P, Sola C, Schmid RD, Valero F (2001) Optimization of the high-level production of Rhizopus oryzae lipase in Pichia pastoris. J Biotechnol 86:59-70.

Moyses C (2003) Substrate reduction therapy: clinical evaluation in type 1 Gaucher disease. Philos Trans R Soc Lond B Biol Sci 358:955-960.

Nakamura S, Takasaki H, Kobayashi K, Kato A (1993) Hyperglycosylation of hen egg white lysozyme in yeast. J Biol Chem 268:12706-12712.

Neufeld EF (1991) Lysosomal storage diseases. Annu Rev Biochem 60:257-280.

Nilsson O, Svennerholm L (1982) Accumulation of glucosylceramide and glucosylsphingosine (psychosine) in cerebrum and cerebellum in infantile and juvenile Gaucher disease. J Neurochem 39:709-718.

Ockerman PA (1968) Identity of beta-glucosidase, beta-xylosidase and one of the beta-galactosidase activities in human liver when assayed with 4-methylumbelliferyl-beta-D-glycosides studies in cases of Gaucher's disease. Biochim Biophys Acta 165:59-62.

Ogrydziak DM (1993) Yeast extracellular proteases. Crit Rev Biotechnol 13:1-55.

Orvisky E, Park JK, LaMarca ME, Ginns EI, Martin BM, Tayebi N, Sidransky E (2002) Glucosylsphingosine accumulation in tissues from patients with Gaucher disease: correlation with phenotype and genotype. Mol Genet Metab 76:262-270.

Paifer E, Margolles E, Cremata J, Montesino R, Herrera L, Delgado JM (1994) Efficient expression and secretion of recombinant alpha amylase in Pichia pastoris using two different signal sequences. Yeast 10:1415-1419.

Pardridge WM (2002) Drug and gene delivery to the brain: the vascular route. Neuron 36:555-558.

Pardridge WM (2006) Molecular Trojan horses for blood-brain barrier drug delivery. Curr Opin Pharmacol 6:494-500.

Pardridge WM (2007) Drug targeting to the brain. Pharm Res 24:1733-1744.

Pelled D, Shogomori H, Futerman AH (2000) The increased sensitivity of neurons with elevated glucocerebroside to neurotoxic agents can be reversed by imiglucerase. J Inherit Metab Dis 23:175-184.

Pelled D, Trajkovic-Bodennec S, Lloyd-Evans E, Sidransky E, Schiffmann R, Futerman AH (2005) Enhanced calcium release in the acute neuronopathic form of Gaucher disease. Neurobiol Dis 18:83-88.

Pentchev PG, Brady RO, Hibbert SR, Gal AE, Shapiro D (1973) Isolation and characterization of glucocerebrosidase from human placental tissue. J Biol Chem 248:5256-5261.

Queiroz JA, Tomaz CT, Cabral JM (2001) Hydrophobic interaction chromatography of proteins. J Biotechnol 87:143-159.

Richins RD, Mulchandani A, Chen W (2000) Expression, immobilization, and enzymatic characterization of cellulose-binding domain-organophosphorus hydrolase fusion enzymes. Biotechnol Bioeng 69:591-596.

Ron I, Horowitz M (2005) ER retention and degradation as the molecular basis underlying Gaucher disease heterogeneity. Hum Mol Genet 14:2387-2398.

Sawkar AR, D'Haeze W, Kelly JW (2006) Therapeutic strategies to ameliorate lysosomal storage disorders--a focus on Gaucher disease. Cell Mol Life Sci 63:1179-1192.

Sawkar AR, Cheng WC, Beutler E, Wong CH, Balch WE, Kelly JW (2002) Chemical chaperones increase the cellular activity of N370S beta -glucosidase: a therapeutic strategy for Gaucher disease. Proc Natl Acad Sci U S A 99:15428-15433.

Schwarze SR, Ho A, Vocero-Akbani A, Dowdy SF (1999) In vivo protein transduction: delivery of a biologically active protein into the mouse. Science 285:1569-1572.

Scorer CA, Buckholz RG, Clare JJ, Romanos MA (1993) The intracellular production and secretion of HIV-1 envelope protein in the methylotrophic yeast Pichia pastoris. Gene 136:111-119.

Shaaltiel Y, Bartfeld D, Hashmueli S, Baum G, Brill-Almon E, Galili G, Dym O, Boldin-Adamsky SA, Silman I, Sussman JL, Futerman AH, Aviezer D (2007) Production of glucocerebrosidase with terminal mannose glycans for enzyme replacement therapy of Gaucher's disease using a plant cell system. Plant Biotechnol J 5:579-590.

Sibille A, Eng CM, Kim SJ, Pastores G, Grabowski GA (1993) Phenotype/genotype correlations in Gaucher disease type I: clinical and therapeutic implications. Am J Hum Genet 52:1094-1101.

Sidransky E (2004) Gaucher disease: complexity in a "simple" disorder. Mol Genet Metab 83:6-15.

Sinclair G, Choy FY (2002) Synonymous codon usage bias and the expression of human glucocerebrosidase in the methylotrophic yeast, Pichia pastoris. Protein Expr Purif 26:96-105.

Sinclair G, Pfeifer TA, Grigliatti TA, Choy FY (2006) Secretion of human glucocerebrosidase from stable transformed insect cells using native signal sequences. Biochem Cell Biol 84:148-156.

Sinclair GB (2001) Mutation analysis, heterologous expression, and characterization of human glucocerebrosidase. In: University of Victoria.

Sinha J, Plantz BA, Inan M, Meagher MM (2005) Causes of proteolytic degradation of secreted recombinant proteins produced in methylotrophic yeast Pichia pastoris: case study with recombinant ovine interferon-tau. Biotechnol Bioeng 89:102-112.

Sorge JA, West C, Kuhl W, Treger L, Beutler E (1987) The human glucocerebrosidase gene has two functional ATG initiator codons. Am J Hum Genet 41:1016-1024.

Sreekrishna K, Brankamp RG, Kropp KE, Blankenship DT, Tsay JT, Smith PL, Wierschke JD, Subramaniam A, Birkenberger LA (1997) Strategies for optimal

synthesis and secretion of heterologous proteins in the methylotrophic yeast Pichia pastoris. Gene 190:55-62.

Stowens DW, Teitelbaum SL, Kahn AJ, Barranger JA (1985) Skeletal complications of Gaucher disease. Medicine (Baltimore) 64:310-322.

Takagi Y, Kriehuber E, Imokawa G, Elias PM, Holleran WM (1999) Beta-glucocerebrosidase activity in mammalian stratum corneum. J Lipid Res 40:861-869.

Tang NL, Zhang W, Grabowski GA, To KF, Choy FY, Ma SL, Shi HP (2005) Novel mutations in type 2 Gaucher disease in Chinese and their functional characterization by heterologous expression. Hum Mutat 26:59-60.

Tayebi N, Stubblefield BK, Park JK, Orvisky E, Walker JM, LaMarca ME, Sidransky E (2003) Reciprocal and nonreciprocal recombination at the glucocerebrosidase gene region: implications for complexity in Gaucher disease. Am J Hum Genet 72:519-534.

Terpe K (2003) Overview of tag protein fusions: from molecular and biochemical fundamentals to commercial systems. Appl Microbiol Biotechnol 60:523-533.

Triguero D, Buciak J, Pardridge WM (1990) Capillary depletion method for quantification of blood-brain barrier transport of circulating peptides and plasma proteins. J Neurochem 54:1882-1888.

Van Den Hazel HB, Kielland-Brandt MC, Winther JR (1996) Review: biosynthesis and function of yeast vacuolar proteases. Yeast 12:1-16.

Verma R, Boleti E, George AJ (1998) Antibody engineering: comparison of bacterial, yeast, insect and mammalian expression systems. J Immunol Methods 216:165-181.

Vervecken W, Kaigorodov V, Callewaert N, Geysens S, De Vusser K, Contreras R (2004) In vivo synthesis of mammalian-like, hybrid-type N-glycans in Pichia pastoris. Appl Environ Microbiol 70:2639-2646.

Vives E, Brodin P, Lebleu B (1997) A truncated HIV-1 Tat protein basic domain rapidly translocates through the plasma membrane and accumulates in the cell nucleus. J Biol Chem 272:16010-16017.

Weinreb NJ, Charrow J, Andersson HC, Kaplan P, Kolodny EH, Mistry P, Pastores G, Rosenbloom BE, Scott CR, Wappner RS, Zimran A (2002) Effectiveness of enzyme replacement therapy in 1028 patients with type 1 Gaucher disease after 2 to 5 years of treatment: a report from the Gaucher Registry. Am J Med 113:112-119.

Yu Z, Sawkar AR, Kelly JW (2007a) Pharmacologic chaperoning as a strategy to treat Gaucher disease. FEBS J 274:4944-4950.

Yu Z, Sawkar AR, Whalen LJ, Wong CH, Kelly JW (2007b) Isofagomine- and 2,5-anhydro-2,5-imino-D-glucitol-based glucocerebrosidase pharmacological chaperones for Gaucher disease intervention. J Med Chem 50:94-100.

Zay A, Choy FY, Macleod P, Tan-Dy CR (2008) Perinatal lethal Gaucher's disease without prenatal complications. Clin Genet 73:191-195.

Zeder-Lutz G, Cherouati N, Reinhart C, Pattus F, Wagner R (2006) Dot-blot immunodetection as a versatile and high-throughput assay to evaluate recombinant GPCRs produced in the yeast Pichia pastoris. Protein Expr Purif 50:118-127.

Zhang XY, Dinh A, Cronin J, Li SC, Reiser J (2008) Cellular uptake and lysosomal delivery of galactocerebrosidase tagged with the HIV Tat protein transduction domain. J Neurochem 104:1055-1064.

Zhang Y, Zhu C, Pardridge WM (2002) Antisense gene therapy of brain cancer with an artificial virus gene delivery system. Mol Ther 6:67-72.